Pan African University
Institute of Water and Energy Sciences

PAN AFRICAN UNIVERSITY
INSTITUTE OF WATER AND ENERGY SCIENCES
(Including CLIMATE CHANGE)

Master Dissertation

Submitted in partial fulfillment of the requirements for the Master degree in

Water Engineering

Presented by

Modou Regis Freddy HOUNDEKINDO

Flood risk assessment in the Niger River Basin in support of the conception of a flood risk management plan: case study of the district of Malanville, Benin

Defended on 04/09/2018 Before the Following Committee:

Chair	Rouissat Bouchrit	Prof.	Tlemcen University
Supervisor	Erik Mosselman	Dr.	Delft University of Technology
External Examiner	Navneet kumar	Dr.	ZEF, University of Bonn
Internal Examiner	Houcine Ziani-Cherif	Dr.	Tlemcen University

DECLARATION

I, **Freddy HOUNDEKINDO**, hereby declare that this thesis represents my personal work, realized to the best of my knowledge. I also declare that all information, material and results from other works presented here, have been fully cited and referenced in accordance with the academic rules and ethics.

Signed  Date: 31/07/2018

HOUNDEKINDO Modou Regis Freddy

CERTIFICATION

This thesis has been submitted with my approval as the supervisor

Signed 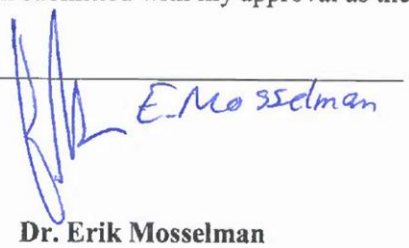 Date 10 September 2018.

Dr. Erik Mosselman

Delft University of Technology, Assistant professor / Researcher / Lecturer

Deltares, Specialist / Expert adviser / Deputy Department head.

ACKNOWLEDGEMENTS

I gratefully acknowledge the African Union for awarding me a scholarship for my studies at the Pan African University.

I sincerely thank my supervisor Dr. Erik Mosselman, for his constant support, time and guidance.

I would like to thank my colleague and friend N'guessan Aimé Konan for his feedback and his support throughout this research

I also want to thank all people and organization who provided data through their online databases for their contribution in this research by sharing their program source and information for use.

Last, but not least, I thank my family for their support and motivation.

Abstract

This thesis was carried out to evaluate the flood risk in the district of Malanville located along the Niger River. The knowledge produce by this study is useful in the implementation of adaptation and/or mitigation measures to alleviate the impact of the flooding on the populations, the economy and the environment. Over the course of the study, the lack of data in the area of interest has been one of the main challenges encountered. Therefore, in the analysis of the flood hazard different sources of remotely sensed data were used.

Moreover, the flood hazard was analysed by applying a 1D hydraulic model HEC-RAS. After setting up the model for the study area, the different flood scenarios considered were simulated and mapped using ArcGIS and HEC-GEORAS extension. The result of the simulation gave information about the inundated areas and the water depths at each location.

From the analysis of the flood hazard, it was found that between 47% and 50% of the total area of the district of Malanville would be flooded in the different flood scenarios considered, and the water depth varies between 1 and 7 m. The townships of Malanville most at risk of flooding are Momkassa and Galiel, located in a high-risk and very high-risk zone, respectively. Furthermore, the assessment of the flood risk showed that the most vulnerable sector to the inundations is the agricultural sector. Indeed, the cultivated floodplains were the most affected areas by the floodwater in every flood scenarios. Knowing that a high proportion of the population of the district relies on their farmlands in these floodplains for their livelihood, the floods pose a challenge not only to the food security in the area but also to its development.

Keywords: HEC-RAS, remote sensing, vulnerability, risk, flood risk management, Niger

Résume

Cette étude a été réalisée afin d'évaluer le risque d'inondation dans l'arrondissement de Malanville situé le long du fleuve Niger. Les connaissances produites par cette étude sont utiles dans la mise en œuvre de mesures d'adaptation et/ou d'atténuation pour mitiger l'impact des inondations sur les populations, l'économie et l'environnement. Au cours de l'étude, le manque de données dans le domaine d'intérêt a été l'un des principaux défis rencontrés. Par conséquent, lors de l'analyse de l'inondation, différentes sources de données de télédétection ont été utilisées.

De plus, l'inondation et ses caractéristiques ont été analysées avec le modèle hydraulique 1D HEC-RAS. Après la mise en place du modèle sur la zone d'étude, les différents scénarios d'inondations considérés ont été simulés et cartographiés en utilisant le logiciel ArcGIS et son extension HEC-GEORAS. Le résultat de la simulation a donné des informations sur les zones inondées et les profondeurs d'eau.

De cette étude, il en ressort qu'entre 47% et 50% de la superficie totale de l'arrondissement de Malanville serait inondé dans les différents scénarios de crue considérée, et la profondeur de l'eau varierait entre 1 et 7 m. Les cantons de Malanville les plus à risque d'inondation sont Momkassa et Galiel. Ils sont en effet situés respectivement dans une zone à haut risque et à très haut risque dans chaque scénario d'inondation considéré. En outre, l'évaluation du risque d'inondation a montré que le secteur le plus vulnérable aux inondations est le secteur agricole. En effet, les plaines cultivées étaient les zones les plus touchées par les inondations. Sachant qu'une grande partie de la population de l'arrondissement dépend de leurs terres cultivées dans ces plaines inondables pour leur subsistance, les inondations constituent un défi non seulement pour la sécurité alimentaire dans la région, mais aussi pour son développement.

Mots clés : HEC-RAS, Télédétection, Vulnérabilité, risque, gestion des risques d'inondation, Fleuve Niger

Contents

List of figures

List of tables

LIST OF ABBREVIATIONS AND ACRONYMS

NBA	Niger basin Authority
INSAE	Institut National de la statistique et de l'analyse économique
RGHP	Recensement General de la Population et de l'Habitation
LDC	Least Developed Countries
NRB	Niger River Basin
DEM	Digital Elevation Model
GIS	Geographic Information System
SRTM	Shuttle Radar Topography Mission
ALOS	Advanced Land Observing Satellite
UNEP	United Nations Environment Programme
UNISDR	United Nations Office for Disaster Risk Reduction
USACE	U.S. Army Corps of Engineers
RS	Remote Sensing
FRM	Flood Risk Management
USGS	United States Geological Survey

CHAPTER 1

1. Introduction

1.1. Background

Flooding is one of the most common natural disasters in the world. Its frequency is indeed higher than the frequency of other catastrophes such as earthquakes, extreme temperature, landslides, drought, wildfire, etc. It is in fact the most recurrent of all environmental hazards and it regularly claims over 20,000 lives per year and affects around 75 million people worldwide (Pitt, 2008). As shown in Figure 1.1 flood is the first water-related disaster affecting people all over the world 1995-2015, and it has been responsible for 8.2% of global disaster deaths 2006-2015 (UNISDR, 2009). Due to the displacement of populations, losses in agriculture and infrastructure, water-related hazards such as floods put a heavy strain on the development of the Least Developed Countries (LDC), undermining previous development efforts (UNISDR, 2016).

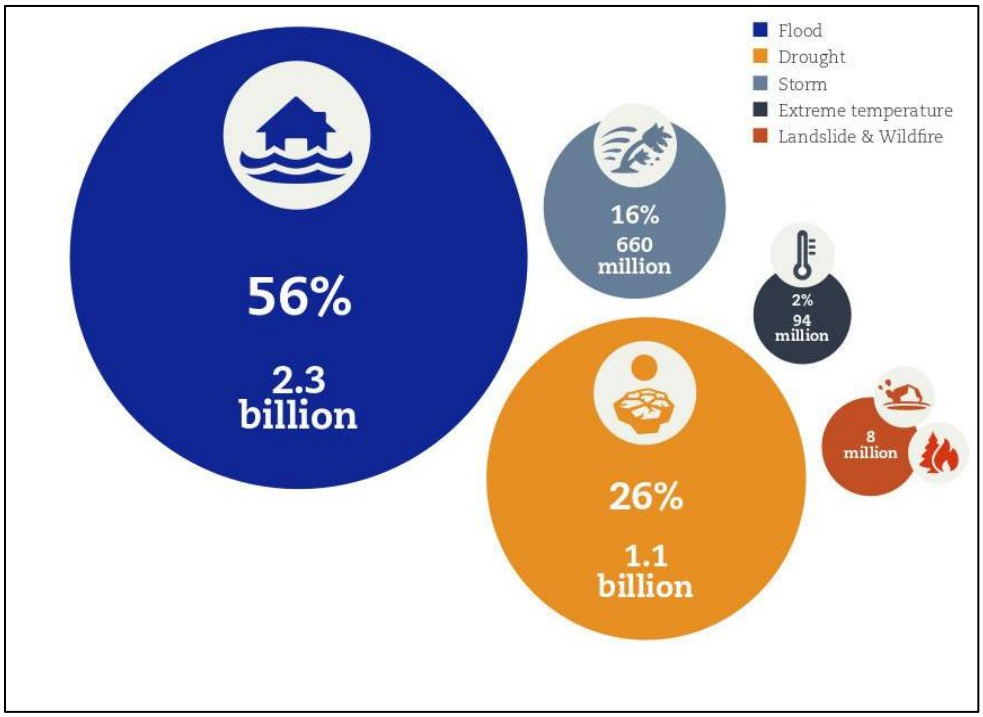

Figure 1.1: Number of people affected by weather-related disasters (1995-2015) (NB: deaths are excluded from the total affected) (UNISDR, 2016)

With a length of 4,200 km, the Niger River is the third-longest river in Africa. It originates on the Guinean Fouta-Djalon Plateau after which it flows through vast flood plains in Mali (the Inner Delta) before resuming its path through Niger and Nigeria into the Atlantic Ocean. Over the past years, several flooding events have affected the population living along the Niger River. The most recent one happened in September 2017 resulting in loss of lives, social disruption and damage to buildings and crops. Before this catastrophe, several floods events have been reported in the area with an enormous impact on the population

living in the Niger River Basin (NRB) exacerbating the poverty-cycle in the region. The flood events of 2009 and 2010 affected 100,000 and 1 million people, respectively. The 2012 flood remains one of the most devastating flood in the region, with more than 10 million people being affected. The riparian country governments' disaster management approach has mostly been focused on the response to and recovery from the catastrophe. Less attention has been placed on mitigation and adaptation measures to limit the impact of the floods on the population. This has left the population highly vulnerable to the disaster over time. Furthermore, the high level of poverty that is prevalent in the region, the lack of effective early warning systems, the poor risk governance and the civil protection mechanisms often intensify the impacts of natural hazards and limit the ability of the population to cope when disaster strikes (Kai et al, 2004).

In recent years, several studies have shown the increase in the frequency and severity of floods in the NRB due to a change in rainfall patterns and land use (Aich *et al.*, 2014; Geo, 2015). Aich *et al.* (2016) have established that there is an increase in the number of people affected by catastrophic floods for the entire NRB. Previous studies have placed greater emphasis on hydrological modeling and rainfall / runoff modeling in the Niger River Basin. Indeed, few studies have analyzed the risk posed by the floods in the region (Behanzin *et al.*, 2016). An understanding of the characteristics of the risk will help in effectively managing the flood risk and thus reduce the damage caused by the hazard on the people and their properties.

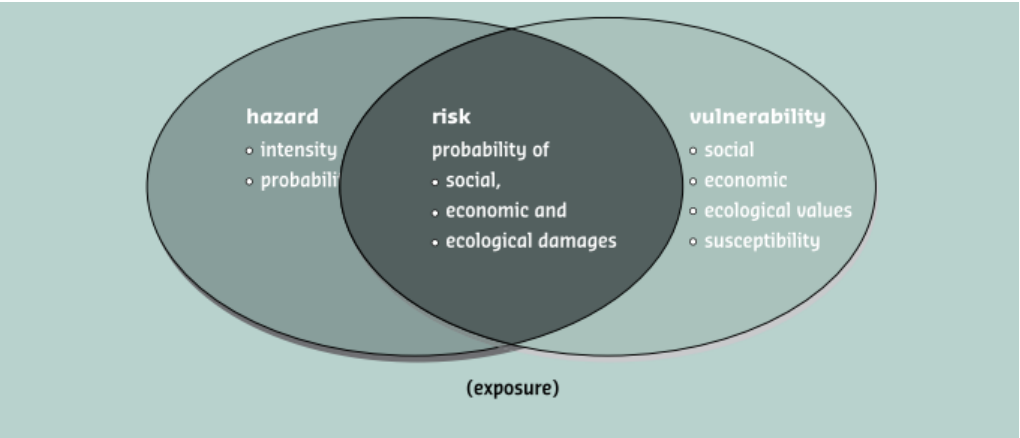

Figure 1.12: Flood risk and its components (Klijn *et al.*, 2009)

Although crucial in the understanding and the evaluation of the flood risk, pertinent data are often not available. Futhermore, time and budget constraints limit the amount and quality of data that can be collected in the field during a research. Those are some of the challenges this thesis was confronted with. Indeed, even though efforts have been made by the riparian countries in this direction, the availability of reliable in situ data is still an issue in the Niger River Basin. Thereby, this thesis had to rely mostly on remotely sensed data for the different analyses performed. Remotely sensed data has the advantage of being readily available

with a good coverage of the study area. Furthermore, several sources of global remote-sensing data useful in a flood risk assessment are freely accessible (DEM, satellite images, etc.).

Malanville, a northeastern district of Benin Republic, is one of the areas located along the Niger River, which suffers the impact of its overflow each year. Over the years, Malanville has known several flooding episodes that have affected the lives of its different communities. Given that the majority of the population in the region rely mostly on agriculture, the cost of the different flooding event in the region has been rather heavy to bear. A sound flood risk management plan is needed in the region and must be supported by an accurate assessment of the flood risk. Risk is defined as the product of the flood hazard (probability and magnitude) and the vulnerability(Klijn *et al.*, 2009). To study the flood risk, each of its components was analyzed and mapped in this work and an overall flood risk map was produced. This work will be an essential part of a flood risk management plan in the district of Malanville located in Niger River Basin (NRB), and the results obtained will provide a scientific base in the planning and decision-making process regarding inundations in the NRB.

Figure 1.1: Niger River basin (source: https://commons.wikimedia.org/wiki/File:Niger_river_map.svg)

1.2 Research Objectives

1.2.1 Overall objective

The overall objective of this thesis is to assess the flood risk in the district of Malanville located in the Niger River basin using remotely sensed data, GIS and hydraulic modeling. The analysis will yield flood hazard maps for different exceedance probabilities and flood risk maps that take into consideration the hazard and the vulnerability of the communities at risk.

1.2.2 Specific objectives

- Flood hazard analysis using statistical frequency analysis and hydraulic modeling
- Assessment of the vulnerability (exposure and socio-economic) of the study area to floods of different return period
- Mapping of the flood risk of the study area for floods of low, medium and high frequency

1.2.3 Research questions

This research will be guided by the following questions:

- What is the exposure of the communities at risk to different flood scenarios (low, medium, high)?
- How vulnerable the communities are to the different floods scenario?
- What type of measure (structural and non-structural) would work best to alleviate the flood risk in the study area?

1.3 Limitations and assumptions

The main limitation encountered in this study was that observed discharge data and topography data in the area of interest could not be acquired.

Thus, the thesis had to rely mostly on remotely sensed data namely ALOS World 3D DEM, Landsat 8 satellite images and simulated discharge to perform the analysis. Even though such data have the advantage of being readily accessible and free, often their low resolution limit the accuracy of the modeling output.

Furthermore, the calibration of the hydraulic model was performed with Landsat images of historical floods. Indeed, no survey was done on the field to gather information on historical floods for the model calibration. This is mainly due to time and financial restriction. Another limitation is that no particular attention has been given to the question of climate change in the assessment of the flood risk.

1.4 Thesis outline

To achieve the objectives mentioned above, this thesis is structured the following way. In Chapter 2, the results of the literature review will be presented including a thorough discussion about concepts relevant to this work. The third chapter will present the area of interest. The fourth chapter will focus on the dataset used for the analysis in this work and the methodology that has been adopted. The result of the analysis is presented in the fifth chapter followed by the discussion. The last chapter is dedicated to the conclusion and recommendations**.**

CHAPTER 2

2. LITERATURE REVIEW

2.1 Introduction

A flood can only be a source of damage when vulnerable human systems are exposed to the hazard.

In this research, three main topics were analysed in order to evaluate the flood risk:

- The probabilities of occurrence and the hydraulic characteristics of different flood scenarios;
- The level of exposure of the population to different return period floods
- The vulnerability of the population at risk.

2.2 Flood Hazard

Flood is broadly understood by the temporal presence of water on an area that is usually dry. From this simple definition two important aspect of flooding are implied: the temporality of the phenomenon and the spatial characteristics. Floods are of mainly 3 types: floods from rivers, mountain torrents, and floods from the sea in coastal areas (Martini and Loat, 2007). According to UNEP (2002), flood is one of the major environmental disasters in Africa with drought. In addition to economic and social damage, floods can have severe consequences, where cultural sites of significant archeological value are inundated or where protected wetland areas are destroyed (Pistrika and Tsakiris, 2007). The lack of effective measure and instrument from government institutions has put the poorest community in a high state of vulnerability to flooding. This explains the high level of damage due to flooding recorded every year during the inundation season. Flood frequency analysis is one of the important studies of river hydrology. It is essential to interpret the past record of flood events in order to evaluate future possibilities of such occurrences. Floods can be categorized according to the speed of the water, geography or cause of flooding.

Table 2.1: Summary of the different types of floods (Source EXCIMAP Handbook on good practices for flood mapping in Europe)

Type of flooding	**Causes of flooding**	**Effect of flooding**	**Relevant parameters**
River flooding in flood plains	- Intensive rainfall and/or snowmelt - Ice jam, clogging - Collapse of dikes or other protective structures	- Stagnant or flowing water outside the channel	- Extent (according to probability) - Water depth - Water velocity - Propagation of flood
Sea water flooding	- Storm surge - Tsunami - High tide	- Stagnant or flowing water behind the shore line - Salinization of agricultural land	- Same as above
Mountain torrent activity or rapid run-off from hills	- Cloud burst - Lake outburst - Slope instability in watershed - Debris flow	- Water and sediments outside the channel on alluvial fan; erosion along channel	- Same as above; - Sediment deposition
Groundwater flooding	- High water level in adjacent water bodies	- Stagnant water in flood plain (long period of flooding)	- Extent (according to probability)

			- water depth
Lake flooding	- Water level rise through inflow or wind induced set up	- Stagnant water behind the shore line	- Same as above

2.3 Flood Routing

Flow routing methods are used to predict the changes in shape of a hydrograph as water travels through a river channel. It is one of the classical problems in applied hydrology. If the flow is a flood, the same technique is used to determine the flood hydrograph (the magnitudes, volumes, and temporal patterns of the flood wave) at a section of a river by utilizing the data of the hydrograph at one or more upstream sections. Flood routing is used in the hydrologic analysis of problems such as flood forecasting and flood protection. Reservoir design and spillway design invariably include flood routing. Numerous technic of flood routing exist (dynamic and diffusion wave models, linear and nonlinear Muskingum models). They can be classified as either hydrologic/Lumped or Distributed/hydraulic.

Lumped/hydrologic

Flow is calculated as a function of time alone at a particular location.

It is governed by continuity equation/storage relationship. In its simplest form, inflow to the river reach is equal to the outflow at the river reach plus the change of storage

$\frac{dS}{dt} = I(t) - Q(t)$ Equation 1

Q and S are unknown.

Distributed/hydraulic

- Combines the continuity equation with some more physical relationship describing the actual physics of the movement of the water.
- Flow is calculated as a function of space and time throughout the system
- Governed by the continuity and the momentum equations

$\frac{\partial v}{\partial t} + V\frac{\partial v}{\partial x} + \frac{g}{A}\frac{\partial(\bar{y}A)}{2x} + \frac{vg}{A} = g(S_o + S_f)$ Equation 2

Momentum equation expressed by considering the external forces acting on a control section of water as it moves down a channel

$S_f = S_o - \frac{\partial y}{\partial x} - \frac{v}{g}\frac{\partial v}{\partial x} - \frac{1}{g}\frac{\partial v}{\partial t}$ Equation 3

Henderson (1966) expression of the momentum equation

2.4 Flood risk assessment

A sound decision-making process in the management of flood risk is bound to go through an estimation of the risk in order to implement effective mitigation/adaptation measures. The concept of risk encompasses both uncertainties and the damages caused by the hazard (Kaplan *et al.*, 1981). However, a distinction should be made between hazard and risk. Indeed, hazard is defined as a source of danger while the risk is the probability that one would face certain losses due to the hazard. Kaplan et al (1981) regarded the risk analysis has a process that consists of an answer to the following three questions:

- What can happen? (i.e., what can go wrong?)
- How likely will it happen?
- If it does happen, what are the consequences?

Flood risk is defined as the probability that a flood of a given magnitude and a given loss will occur within a given time span (Thieken and Merz, 2006). Likewise, The European Flood Directive defines flood risk as the combination of the probability of a flood event and of the potential adverse impacts on human health, the environment, cultural heritage and economic activity associated with a flood event (Martini and Loat, 2007).

Although being a natural process, humanly impossible to control, a reliable assessment of the flood risk in a river basin is crucial for the implementation of effective measures that limit the impact of the hazard on the people and their assets. Therefore, a flood risk assessment goal is to first identity the probability of occurrence of the hazard and its magnitude (The geographical extent; the depth and duration the velocity of the flood). Through the analysis of the flood hazard, the characteristics of all possible floods, small and frequent as well as big and rare are quantified. However, In order to be thorough a flood risk analysis must include the assessment of the impacts of flooding on the people and their assets taking into account their sensibility to the hazard and their adaptive capacity (Thieken and Merz, 2006). A flood risk assessment seeks to identify locations that are more susceptible to flooding and to understand the source of the risk in

order to design the right measures and instruments that are adapted to the area. A flood risk assessment is vital to support the mitigation or/and prevention of the damages; raise awareness among inhabitants in the vulnerable area; support and manage emergencies in time or avoid building in flood-prone areas (GWP, 2007). In this work, risk assessment refers to the estimation of the probability of occurrence of the hazardous phenomenon and its magnitude and the assessment of the vulnerability of the population to the hazard.

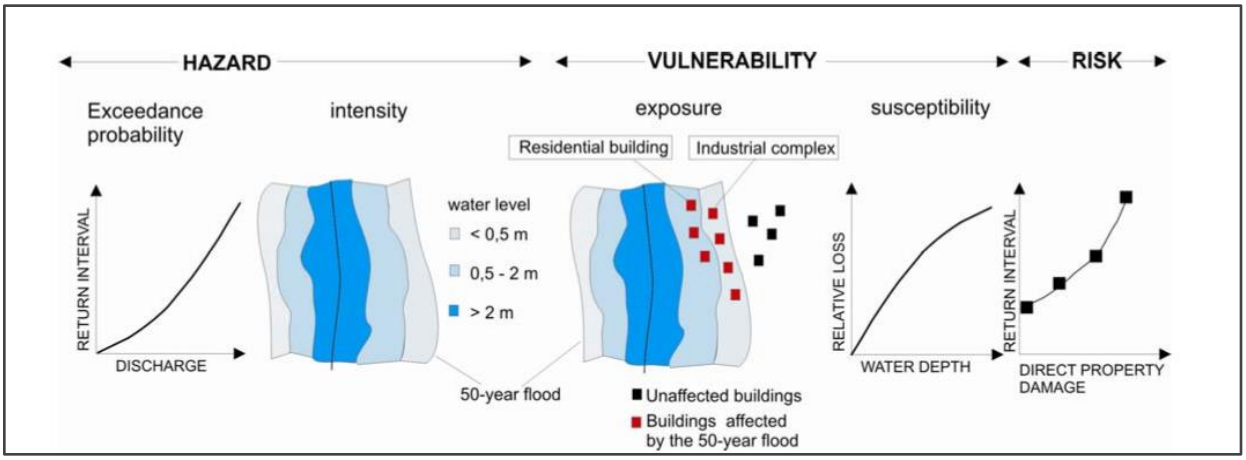

Figure 2.1: Flood risk as interaction of hazard and vulnerability, source: Thieken et al (2014)

2.5 Vulnerability

On its own, information about the flood hazard (it magnitude and its frequency) does not show entirely the extent of the consequences of the flood. In order for a flood of a certain magnitude to pose a risk, the population and the properties must be exposed and vulnerable to the hazard (Klijn *et al.*, 2009). Thereby, the analysis of flood risks must take into account the different aspects of the factors that affect the risks , e.g. human, social, economic and environmental (MESSNER and MEYER, 2005).

Over the years, many schools of thought have emerged around the concept of vulnerability. Recently one school is gaining in significance in the scientific community. It considers vulnerability not only related to the exposure to biophysical hazards but also to the social context of hazards and relates (social) vulnerability to coping responses of communities.

UNISDR (2009) defines the vulnerability of a community as "a set of conditions and processes resulting from physical, social, economic and environmental factors, which increase the susceptibility of a community to the impact of hazards" (UNISDR, 2009)

According to Tsakiris (2014), vulnerability assessment in flood-prone areas depends on the following factors:

- The degree of exposure of the system.
- the initial condition of the system
- the magnitude of the extreme event
- the social factor

The interplay of these factors produces different patterns of vulnerability (Nardo et al, 2014) . Without exposure there is no risk, thus the assessment of the exposure of a community to the hazard is one important step of the vulnerability assessment. The concept of sensitivity and adaptive capacity encompasses socio-economic factors such as gender, age, means of livelihood, income, access to drinking water, etc. Those factors can either increase or decrease the level of vulnerability of the receptor. Vulnerability assessment is often synonymous with vulnerability mapping given that most of the factors that influences the vulnerability of a community are spatially differentiated (Chai-onn, 2015). The United Nations Environment Programme (UNEP) highlights "measuring and mapping vulnerability" as a first priority for supporting adaptation decision-making.

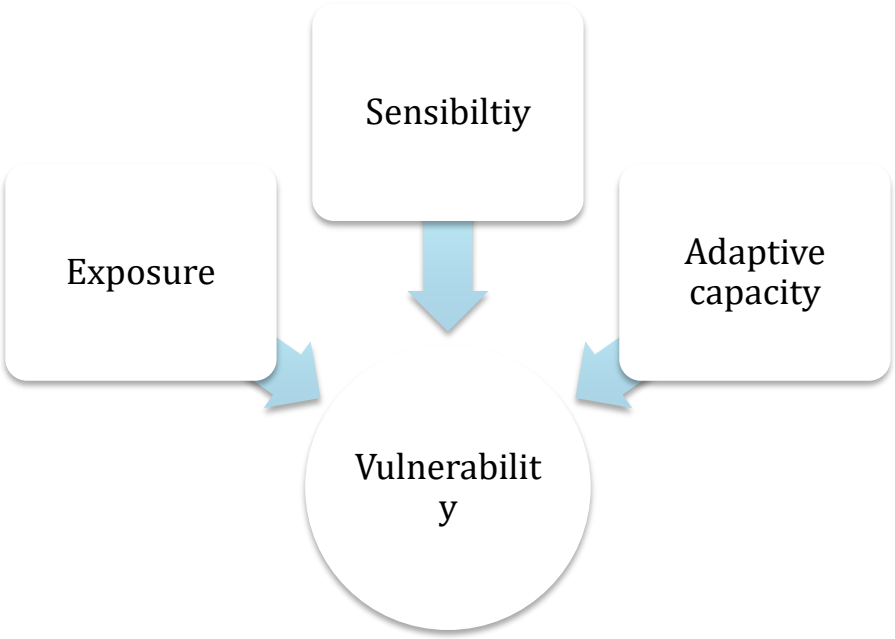

Figure 2.2: The component of vulnerability (Sayers *et al.*, 2013)

2.6 HEC-RAS and HEC-GEORAS

HEC-RAS is a hydrodynamic model developed by the Hydrologic Engineering Center of the US Army Corps of Engineers. The hydraulic model offers both one and two-dimensional hydraulic modeling capacity. HEC-RAS is widely used to simulate flood routing in river systems (Hicks and Peacock, 2005; Timbadiya et al, 2011; Mai and De Smedt, 2017).

This hydraulic model solves the full dynamic Saint-Venant equations through single, dendritic or looped systems of natural and constructed open channels, including overbank/floodplain areas, levee failures, spillways, and overflow structures, and so forth. The combination of free hydrodynamic model such as HEC-RAS and global remotely sensed data provide a cost effective solution for the assessment of the flood risk. Over the years, many studies have shown the strengths and the limitation of HEC-RAS to model floods. Flood-prone areas with different return periods were determined over a 16 km length of the Lighvan Chai River using GIS and HEC-RAS model. The study showed that it is possible to determine the flood area and allowable limit of construction and the criteria for zoning flood and flood insurances by integrating remote sensing data, field study and software such as HEC-RAS (Khaleghi, Mahmoodi and Karimzadeh, 2015). The HEC-RAS (Hydrologic Engineering Center - River Analysis System) modelling framework was used to evaluate both the flood routing and water flow activity of the Ogunpa River. The HEC-RAS model has been able to identify those particular sections of the Ogunpa river course that are susceptible to high water elevation levels and head(Adewale, P. O., Sangodoyin, A. Y., 2011). Mai and De Smedt combined hydrological (WetSpa) and hydraulic model (HEC-RAS) to predict flood in Vietnam. The model was resourceful in the development of a flood forecasting and early warning systems to mitigate losses due to flooding in Vietnam (Mai and De Smedt, 2017).

HEC-RAS was designed to perform one-dimensional, two-dimensional or combined 1D and 2D hydraulic modeling for a full network of natural and constructed channels. The hydraulic model is capable of performing steady flow water profile calculation and unsteady flow routing. HEC-RAS computes the water surface profile from one cross section to another by solving the energy equation with an iterative procedure called the standard step method. The energy equation is written as follows:

$Z_2 + Y_2 + \frac{a_2 V_2^2}{2g} = Z_1 + Y_1 + \frac{a_1 V_1^2}{2g} h_e$ Equation 4

Where: $Z_1, Z_2 = elevation\ of\ the\ main\ channel\ inverts$

$Y_1, Y_2 \quad = depth\ of\ water\ at\ the\ cross\ sections$

$V_1, V_2 \quad = average\ velocities\ (\frac{Total\ discharge}{Total\ flow\ area})$

$a_1, a_2 \quad = velocity\ weighting\ coefficients$

$g \quad = gravitational\ acceleration$

$h_e \quad = energy\ head\ loss$

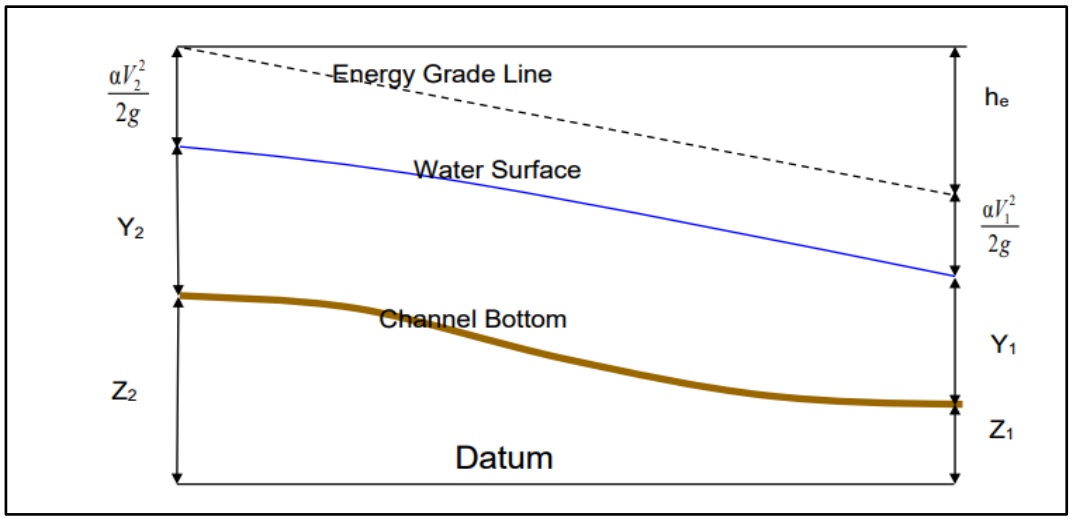

Figure 2.3: representation of terms in the energy equation ((USACE, 2016)

The modeling process used in this study is based on the one-dimensional (1D) approaches. In this model, the river geometry is represented by a series of discrete cross-sections perpendicular to the flow direction. The basic data requirement to run HEC-RAS (Eleuterio, 2012) are:

- Topographic data for the construction of the cross-sections cut lines and the inundation maps
- Manning n coefficient (roughness coefficients)
- The boundary conditions at the upstream and the downstream end of the river reach
- Calibration and validation data (satellite image of historical flood or observed flood depth)

HEC-GEORAS was specifically developed to process geo-spatial data for use with the Hydrologic Engineering Center River's Analysis System (HECRAS). HEC-GEORAS offers a set of procedures, tools, and utilities for the preparation of GIS data to be imported into HEC-RAS and generation of GIS data from RAS output (http://www.hec.usace.army.mil/software/hec-georas/downloads.aspx). During the data preparation, HEC-GEORAS helps to effectively build the river geometry and extract from the DEM the elevation data needed for the cross-sections. Once the modeling of the floods is done with HEC-RAS, the result can be exported to ArcGIS for further analysis with HEC-GEORAS.

Hydraulic modeling offers a rather objective way to model flood. Given that, this modeling method takes into account spatially distributed characteristics of river basins such as the friction coefficient and the riverbed geometry.

2.7 Flood risk assessment and Geospatial techniques

Geospatial techniques which is the suite of geographic information systems (GIS), remote sensing (RS), global positioning systems (GPS), and spatial analysis have demonstrated their potential over the year in the management of natural hazards (Dewan, 2013). Indeed Geographic information systems (GIS) supports the spatial decision making process, by providing tools for creating, storing, analyzing and managing spatial data and associated attributes of the real world. Cartographic aspects are important issues in flood mapping. GIS provides a broad range of tools in flood risk management for the determination of flood-prone areas and the mapping of vulnerability. GIS tools are currently used at each step of the flood risk assessment, from the preparation of the data to the delineation of the floodplain.

Remote sensing (RS) is the science and art of acquiring information (spectral, spatial, and temporal) about material objects, or areas, without coming into physical contact with the objects or areas, under investigation (Lillesand, 2004). In the process of flood risk management, RS has proven to be very efficient in the instantaneous mapping of the flood extent by the acquisition of high-resolution satellite images. RS provides a cost and time effective alternative to in situ data collection in order to build the databases needed in the hazard management. The application of both GIS and RS opens a completely new realm of possibility in the process of flood risk management (MESSNER and MEYER, 2005).

2.8 Flood risk management

Risk cannot be eliminated completely. The only alternative is its management (Connelly, Carter and Handley, 2015).

Flood management has three distinct goals (Martini and Loat, 2007):

- To prevent the further build-up of risks through appropriate and risk-conscious development (i.e. development in safe places, appropriate forms of construction etc.)
- Reduce existing risks through preventive and preparedness measures (e.g. construction of flood dikes and implementation of early warning systems)
- To adapt to changing risk factors (e.g. climate change adaptation)

The flood risk management plan must be implemented in a way that finds an optimal tradeoff between the cost of the measures and the potential damages, with the right mix of structural and non-structural measures (Klijn *et al.*, 2009). Structural measures take in account the construction of protective works such as flood storage reservoir, diversion of water to side channels storm channels, levees along the floodway. Meanwhile, nonstructural measures are concerned with the zoning and the redevelopment of flood-prone areas, flood forecasting and early warning systems. Although non-structural measures

improve the preparedness to floods and reduce losses, the necessity of structural measures would always remain for minimizing the extent of physical damage caused by floods (Udani and Mathur, 2016). It is essential to establish the flood risk management plan on a sound technical and scientific basis. Flood risk management implementation without sufficient risk information can lead to either too little or too much protection rendering the implemented measures ineffective (Wright, 2015).

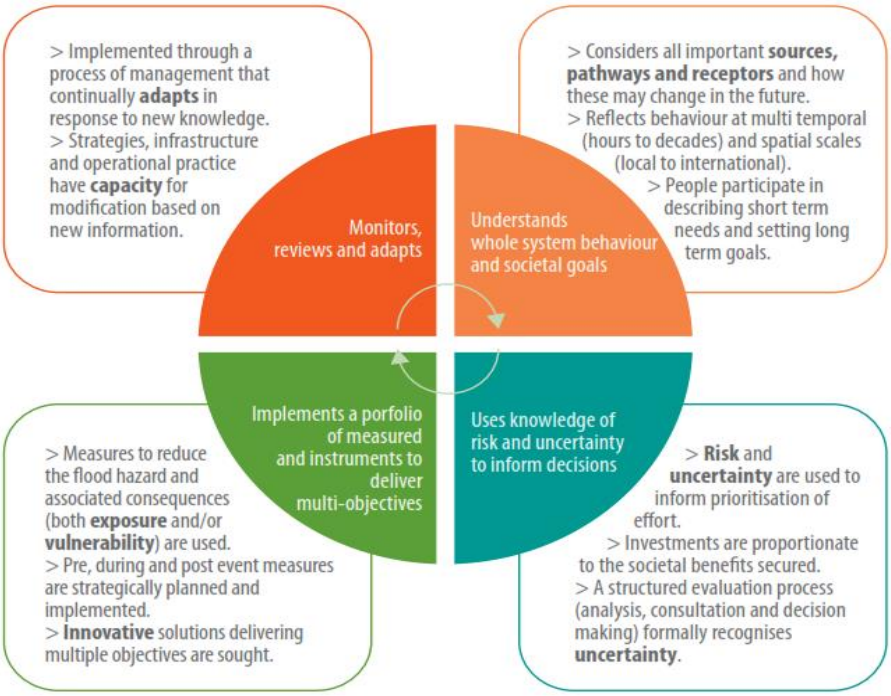

Figure 2.4: The component of a good flood risk management (Sayers *et al.*, 2013)

CHAPTER 3

3. STUDY AREA

3.1 Introduction

The district of Malanville is situated in the Department of Alibori in the northeast of Benin Republic. It lies on the right bank of the Niger River. The proximity to the Niger River, exposes the district to frequent flooding. Malanville covers an area of 183 km² and the average altitude is 200m above sea level. The townships of Malanville are Bodjecali, Galiel, Koki, Tassi-Tedji, Tassi-Zenon, Wollo, Wouro-Hesso, and Momkassa. The district is bounded to the north by the Niger River, the district of Guene to the south, the district of Toumbouctou at the west and the district of Garou on the East. Malanville is one of the district of the municipality of Malanville. The population relies mainly of agriculture for their livelihood and the main cultivated crops are rice, onions, peanuts and tomatoes.

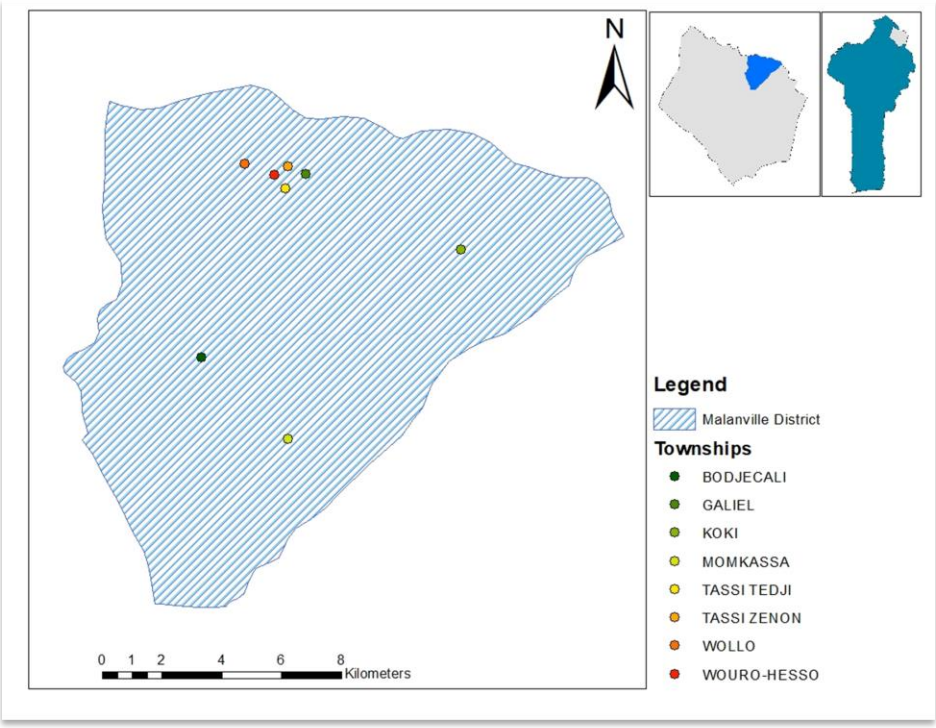

Figure 3.1: Location map of Malanville district

3.2 Climatic Features

Malanville is located in the Sahelo-Sudanian region, which is a semi-arid zone with a dry season from November to April. The dry season is characterized by the "Harmattan" wind flow and temperatures ranging between 12°C and 25°C. The district knows only one rainy season, which lasts 5 to 6 months from May to October with an average annual rainfall between 700 mm and 900 mm. Malanville experiences extreme seasonal variations in monthly rainfall.

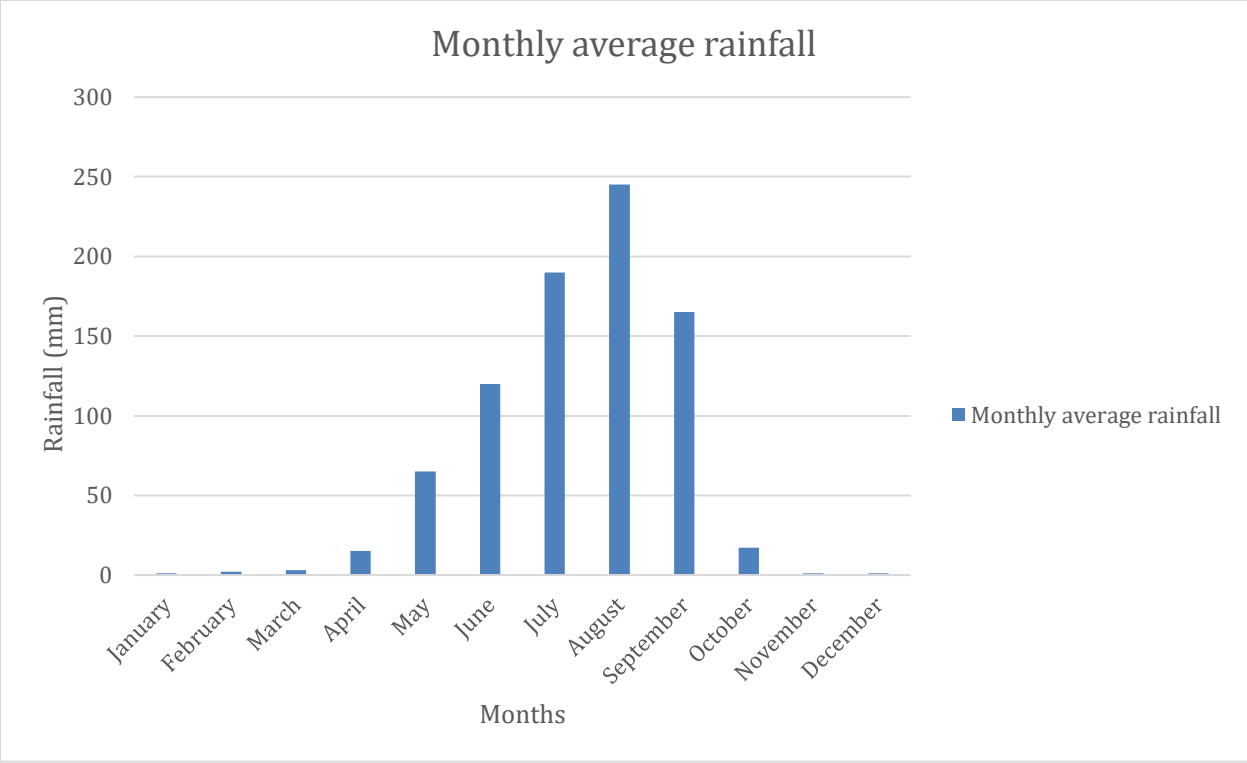

Figure 3.2: Monthly average rainfall of the district of Malanville

Figure 3.2 shows that the months of July, August and September are the wettest of the year.

3.3 Soil Type

The district of Malanville is covered with gneissic soil and in the Niger Valley and its tributaries; there is sandy and ferruginous clay.

3.4 Hydrography

The district of Malanville is located in the Niger Valley. It is crossed from its East to the West by the Niger River, which floods during the months of August and September. The Niger River stretches about 120 km along the Benin border. “La Sota”, with a length of 254 Km crosses the district of Malanville entirely in the North-South-East direction and drains an area of approximately 13,410 Km^2.

3.5 Socio-economic background

3.5.1 Population dynamic

With 68670 inhabitants, Malanville is the most populated district of the municipality of Malanville (INSAE, 2014). This population is concentrated on an area of 183 km² and almost 70% of the population lives in rural areas. In the district of Malanville, out of 1000 children born alive 148 die before reaching their fifth birthday (INSAE, 2015). The mortality level is higher in rural areas than in the urban environment.

3.5.2 Literacy and School Attendance

The literacy rate over 15 years old is round 18% in 2013, which is low. In 2013, 25.8% of children of Malanville between the ages of 6-11 attended school. The net enrollment rate in Malanville is well below the national level (65%). The net secondary school enrollment rate is 15% in 2013. Some progress was made between 2002 and 2013 in terms of schooling but not as significant as between 1992 and 2002.

3.5.3 Religion and Socio-Cultural Groups

The dominant religion in the district of Malanville is Islam. It is practiced by 91.9% of the population while Catholicism is practiced by 3.1%, traditional religions (1.4%), Protestantism (0.6%,) and Other religions (3.1%). The ethnic groups commonly encountered are the Bariba and related (37.1%), Peulh or Fulani (26.5%), Dendi and related (20.1%). The most spoken language is Dendi.

3.5.4 Community Infrastructure

With eight townships, the district of Malanville has four health centers. Access to drinking water seems to pose enormous difficulties to the population. Barely 39% of households have access to drinking water according to the National Statistic Institute of Benin (INSAE). The main sources of water in the district of Malanville are wells and boreholes equipped with water pumps.

3.5.5 Economic Activities of the District

The most dominant branches of activity in the different communities of Malanville are Agriculture and Cattle-breeding. Indeed 37% of the active population of the district rely on agriculture and livestock for their livelihood. Meanwhile, the rest of the population are invested in trading, catering, accommodation and other services. Non-monetary poverty (based on characteristics of habitat and household assets) affects 23.5% of the population of Malanville in 2013. Moreover, 95% of the population between 15 years and 60 years works in the informal sector.

3.5.5.1 Agriculture

Agriculture is the main source of revenue for the district; smallholdings with limited resources characterize it. The agriculture in the district is of an extensive type.

The district of Malanville produces different types of crops namely:

- Cereal crops: Maize, rice, Sorghum, millet
- Vegetable: Onion, tomato, pepper and Okra
- Tubers: Potatoes, cassava, yam
- Cash crops: Cotton, oil palm trees, Peanut, cashew

The predominance of cash crops on food crops raises the question of food security in the district. In fact, a large number of agricultural producers are forced to sell cotton or onion before building up their necessary food stocks for the year.

3.5.5.2 livestock

Livestock occupies a prominent place among the district economic activities. The species raised are mainly cattle, small ruminants and the poultry. The stock raising of goats and pigs has increased significantly. Livestock products are meat, milk, eggs and cheese.

CHAPTER 4

4. MATERIALS AND METHODS

This chapter will provide information about the datasets used to answer the research questions outlined in Chapter 1 and present the methodology adopted in this study.

4.1 Datasets

The data used in this study are of three types:

- Remotely sensed data (DEM and satellite images)
- Census data and
- Discharge data.

Accurate digital maps and digital elevation models (DEM) are important to develop realistic representations of the extent and depth of flooding, particularly where floodplains are relatively flat. The vertical and horizontal accuracy of the maps will have a significant impact on the reliability and the accuracy of the flood maps produced. Landsat 8 satellite images are available on the USGS Earth Explore server (https://earthexplorer.usgs.gov/), the Data products were downloaded from this server. The hydrological catchment model HYPE was adapted to the Niger River Basin to study the potential effects of climatic changes on floods, droughts and other water-related phenomena; and to connect this to adaptation strategies in West Africa. The model was used to simulate daily flow data covering the entire Niger River Basin from 1980 to 2009. The flow data used in this research were acquired from the HYPE platform.

4.1.1 Landsat 8

With over 40 years of activity, The Landsat Program has provided high spatial resolution data of the Earth's surface to a broad and varied user community. The data from the Landsat different spacecraft is until date the longest record of the Earth's continental surfaces as seen from space. Launched on 11 February 2013, Landsat 8 is the most recent satellite of the Landsat Program. The overall mission objectives of this new spacecraft of the Landsat program are (USGS, 2016):

- To provide data continuity with Landsat 4, 5, and 7.
- To offer 16-day repetitive Earth coverage, an 8-day repeat with an L7 offset.
- To build and periodically refresh a global archive of Sun-lit, substantially cloud-free land images.

Landsat 8 follows the same Worldwide Reference System (WRS) used by Landsat 4, 5, and 7, bringing the entire world within view of its sensors once every 16 days. However, combined with Landsat 7, the repeat cycle is shorted to 8 days. Landsat 8 data are downlinked and processed into standard products within 24 hours of acquisition, making it available rapidly to the public. As shown on the Figure 4.2 below, the

Landsat 8 mission carries two instruments on board an Operational Land Imager (OLI) and a Thermal Infrared Sensor (TIRS). OLI acquires data in nine shortwave bands at spatial resolutions of both 30 m (8 bands) and 15 m (1 band). TIRS has two long wave thermal bands, both with 100 m resolution.

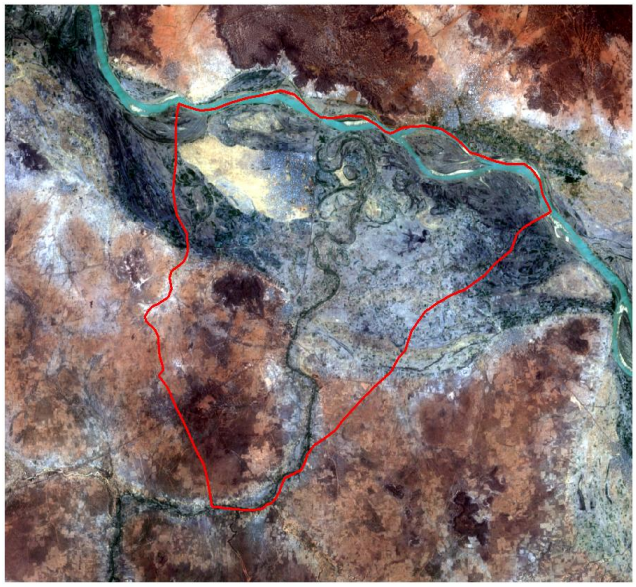

Figure 4.1: Landsat 8 image of the district of Malanville

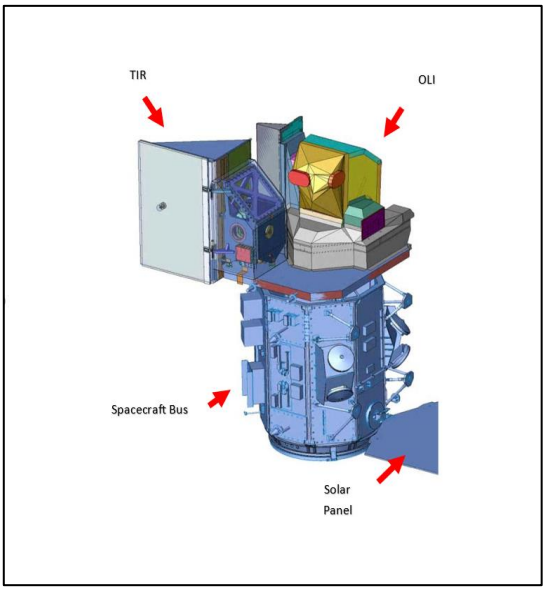

Figure 4.2: Illustration of Landsat 8 Observatory

4.1.2 Topographic Data

Topographic data is one of the most important datasets in flood inundation modeling. The availability of global coverage digital surface models has had a positive impact on scientific researches over the past decade as they provide a fairly good base dataset with a low production time and expense(Józsa et al, 2014). In a region that lacks detailed topographic maps, global coverage digital surface models remain the best source of topographic data for earth science studies. Several DEM are indeed available freely online namely the Shuttle Radar Topography Mission (SRTM), the Advanced Spaceborne Thermal Emission and Reflection Radiometer (ASTER) Global Digital Elevation Model (GDEM) and the ALOS Global Digital Surface Model "ALOS World 3D - 30m (AW3D30)". The latter was used as source of topographic data in the analysis of the flood hazard.

The ALOS Global Digital Surface Model results from the effort of the Japan Aerospace Exploration Agency (JAXA) to develop a precise global digital elevation model that can represent land terrains with approximately 5-meter in spatial resolution and 5 meters in-target height accuracy (standard deviation). The ALOS World 3D-30m (AW3D30) is converted from the AW3D DSM dataset (5-meter mesh) and is

available free of charge since May 2015. This dataset is highly expected to be useful for scientific research and education that needs geospatial information. The DSM dataset covering the research area were downloaded from the Japan Aerospace Exploration Agency (JAXA) platform (http://www.eorc.jaxa.jp/ALOS/en/aw3d30/index.htm) and projected in WGS 1984 UTM Zone 31N.

The Advance Land Observing Satellite (ALOS) has three remote-sensing instruments:

- The Panchromatic Remote-sensing Instrument for Stereo Mapping (PRISM).
- The Advanced Visible and Near Infrared Radiometer type 2 (AVNIR-2).
- The Phased Array type L-band Synthetic Aperture Radar (PALSAR).

The data captured by the Panchromatic Remote-Sensing Instrument for Stereo Mapping PRISM provides a highly accurate digital surface model (DSM). PRISM is a panchromatic radiometer with 2.5 m spatial resolution. The DSM are posted on a 1 arc-second (approximately 30–m) grid and in GeoTIFF format. Digital Elevation Model is a good source of auxiliary information, and it is often used to support flood-mapping techniques (Forkuo, 2013).

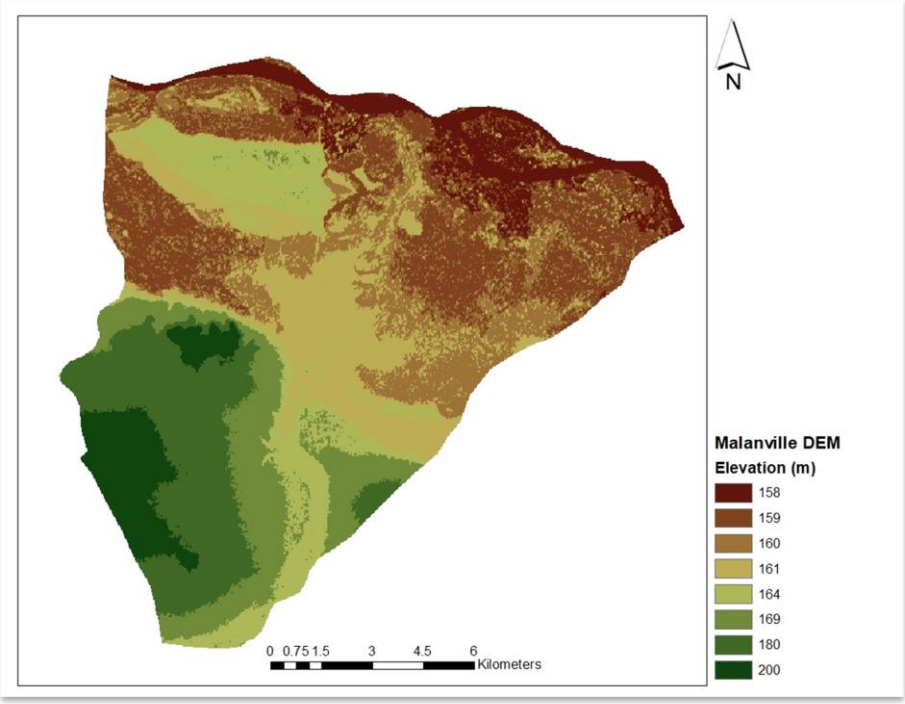

Figure 4.3: Elevation range in the district of Malanville (DEM)

4.1.3 Flow data

The flow data were obtained from the Niger-HYPE project platform. The data are available for each sub-basin of the NRB in excel spreadsheet.

The hydrological catchment model (HYPE) developed by the Swedish Meteorological and Hydrological Institute (SMHI) was adapted to the Niger river basin to study the potential effects of climatic changes on floods, droughts and other water-related phenomena; and to connect this to adaptation strategies in West Africa (http://hypeweb.smhi.se/nigerhype/about/). The model was used to simulate daily discharge at each sub-basin of the entire NRB. The discharge data span from 1980 to 2009 and are available at this link: http://hypeweb.smhi.se/nigerhype/time-series/.

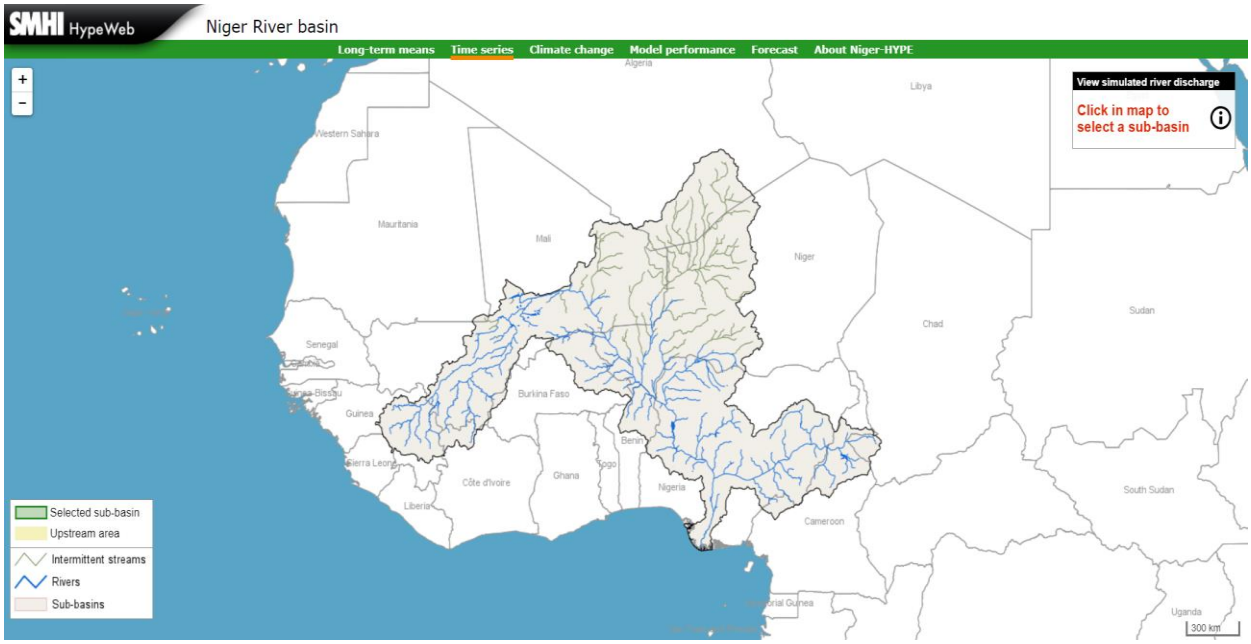

Figure 4.4: Portal of the Niger-HYPE project dataset

4.2 Methodology

The methodology adopted in this study is comprised of four main tasks.

- (1) Data preparation and model setup
- (2) Hydrodynamic modelling and flood hazard mapping
- (3) Vulnerability assessment and vulnerability mapping using ArcGIS
- (4) Flood risk mapping and analysis

4.2.1 Data preparation and model setup

4.2.1.1 Remotely sensed data

Preceding the acquisition of relevant datasets, all the remotely sensed data downloaded were first projected into the appropriate geographic coordinate system (WGS_1984_Zone_31N). Afterwards, the raster data were clipped to the study area. The sinks present in the DEM were filled by using spatial analysis tools from the ArcGIS toolbox. Sinks in elevation data are most commonly due to sampling effects and the rounding of elevations to integer numbers.

4.2.1.2 River Geometry

The preparation of the river geometry was performed using the Hec-GeoRAS extension in ArcGIS. First, the DEM of the study area was converted to a Triangular Irregular Network (TIN) and with Hec-GeoRAS functionalities, the digitization of the channel network and cross-section were performed. During the Digitalization process, a Landsat 8 image of the study area acquired on the 17 Avril 2018 was overlaid on the TIN in order to accurately draw the stream centerlines, the riverbanks and the flow path. As for the cross section cut lines, they were drawn from left to right, from the perspective of looking downstream and perpendicular to the stream centerline (River) to meet the recommendation of the HEC-GeoRAS user manual (Ackerman, 2011). Due to time and financial constraints no field measurements at the sites of application were done to gather information on the channel morphology. Such information was extracted from the generated TIN.

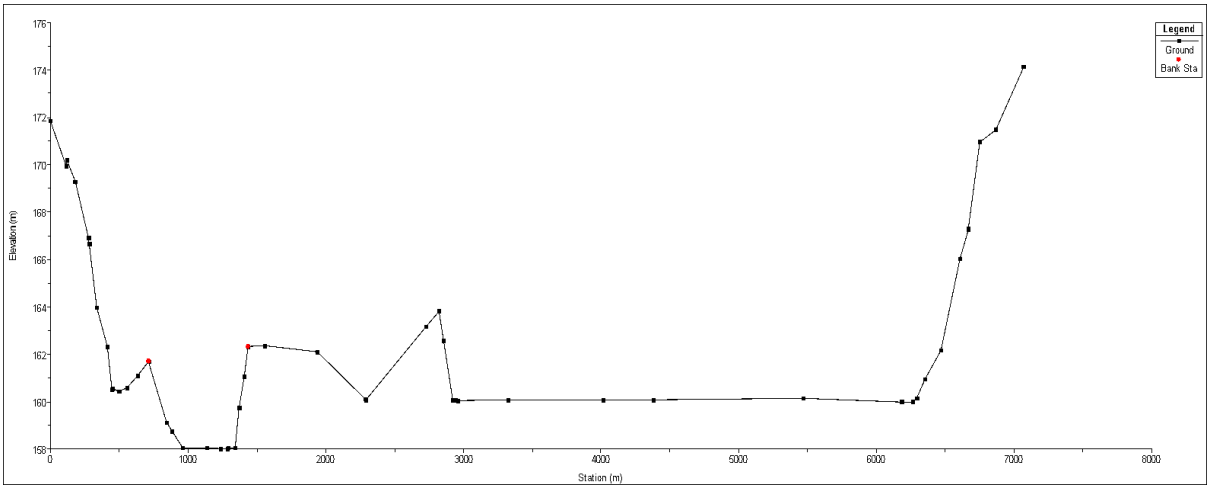

Figure 4.5: example of drawn cross-section profile

Additionally, the cross-section cut lines were extended across the floodplain. Here, the first estimation of the floodplains was performed by analyzing satellite images of historical floods.

4.2.2 Channel Roughness

The roughness parameters (Manning's Roughness coefficient) cause energy loss during flows along a river, leading to the attenuation of the flood wave (Mukolwe, 2016). Channel roughness is a sensitive parameter in the development of a hydraulic model. It is a highly variable parameter, which depends upon a number of factors like the surface roughness, the vegetation, the channel irregularities, the channel alignment, etc. The channel roughness is not a constant parameter and it varies along the river depending upon variation in channel characteristic along the flow (Timbadiya et al, 2011). In this work, the different Manning's coefficients were assigned based on the land use types. A land use/land cover map was conceived using Landsat 8 images. Each of the land use types were allocated a Manning coefficient with reference to Chow (1959). Afterwards, using HEC-GeoRAS functions the manning n values were extracted from the land use tables. The geometry data was then exported to RAS and corrected.

4.2.3 Flood Frequency Analysis

To better characterize the flood hazard, it is necessary to capture both its frequency and its magnitude. In this thesis, the main approach used in the estimation of the return periods and the probabilities associated with each of the required scenarios was the statistical analysis method based on simulated historical data. The probability of a flood scenario characterized as the chance that it will occur in any one year (its annual probability) (Klijn *et al.*, 2009). The probabilistic approach tends to assume that events in the future are predictable based on the experience of the past (Pistrika and Tsakiris, 2007). The return period was determined by examining the record of flood events in the past, using statistical interpolation methods. The available discharge data for the Niger River and the Sota River (tributary) covers a period of 30 years. In order to extrapolate return periods longer than the flow dataset, different probability distributions (Gumbel, Generalized Extreme Value and exponential) were fitted to the dataset. Subsequently, the goodness of fit was assessed by Quantile-Quantile plotting between the hydrologic data and the fitted probability distribution. Extreme value distributions are often used to model the smallest or largest value among a large set of independent, identically distributed random values representing measurements or observations.

4.2.3.1 Gumbel Distribution

The Gumbel distribution is the most widely used distribution to model extremes in hydrology (Koutsoyiannis, 2004). The Gumbel's distribution equation and the procedure for a T return period is given as follows,

$$X_T = \bar{X} + K.\sigma_x \qquad \text{Equation 5}$$

Where:

σ_x: The standard deviation of the Sample Size

K: Frequency Factor, which is expressed as, $K = \frac{Yt - \overline{Yn}}{Sn}$ Equation 6

Yt: Reduced Variate, $Yt = -[\ln \ln \left(\frac{t}{t-1}\right)]$ Equation 7

The values of $\overline{Yn}$ And Sn are selected from Gumbel's Extreme Value Distribution considered depending on the sample size.

4.2.3.2 Generalized Extreme Value

The Generalized Extreme Value combines three simpler distributions into a single form, allowing a continuous range of possible shapes that includes all three of the simplest distributions.

4.2.3.3 Exponential

The exponential distribution is special because of its utility in modelling events that occur randomly over time. The exponential probability density function is

$y = f(x|\mu) = \frac{1}{\mu} e^{\frac{-x}{\mu}}$ (4) Equation 8

μ is the parameter of the distribution.

4.2.4 Hydrodynamic Modeling and flood hazard mapping

Once the River geometry file was imported to HEC-RAS, the next step consisted of entering the hydrologic data and the boundary conditions.

The discharge data obtained from the frequency analysis was used as flow data in the model and a steady flow simulation was performed for each return period considered in this study. Moreover, HEC-RAS proposes four boundary condition options for the steady flow simulation: (1) the known water level, (2) the critical depth, (3) the rating curve and (4) the normal depth. The choice of the boundary condition depends on the data availability. Therefore, the lack of data in the study area led to the choice of the critical depth as boundary condition at the upstream and downstream of the modeled reaches. The model was ran in the subcritical flow regime and the result of the simulation was then exported to ArcMap for the flood hazard mapping using the post processing modules of HEC-GEORAS extension. Lastly, the calibration and validation of the model was performed on the Manning's n coefficient by comparing the modelling results of the flood event of 2013 and 2017 with Landsat 8 images of the same historical floods.

4.2.5 Vulnerability Assessment

Vulnerability is one of the significant components in risk management and flood damage assessment (Koutsoyiannis, 2004). Vulnerability is the degree to which a system is susceptible to, or unable to cope with, the adverse impact of a hazard. The vulnerability of an element at risk is dependent on three

components: the exposure, the sensitivity, and the adaptive capacity. The assessment of the vulnerability of the district of Malanville was performed by analyzing each of the components of vulnerability.

4.2.5.1 Exposure

Exposure refers to the inventory of elements in an area in which hazard events may occur (UNISDR, 2009). The evaluation of the exposure of the population and the asset at risk in Malanville was performed by estimating the number of people and infrastructure that are located in the flooded areas for each flood scenario. This analysis was done by overlaying a recent land use and land cover map of the study area with the flood hazard maps and then estimating the total area of each land use type submerged by the floodwater.

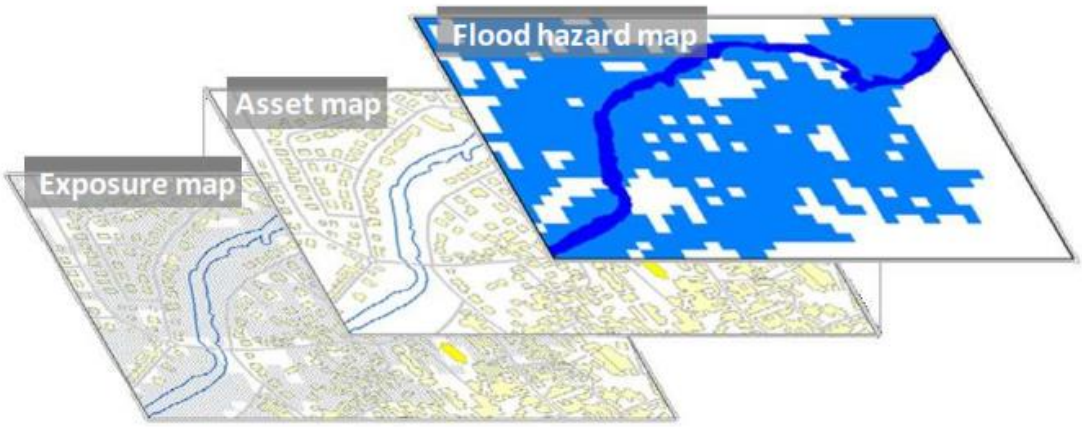

Figure 4.6: Exposure map resulting from the overlaying of the flood hazard map and the asset map (Eleuterio, 2012)

4.2.5.2 Adaptive Capacity and Sensibility

Several studies have shown that even though exposure is an important determinant of the vulnerability of a community, alone, it is not enough to understand the trends in the disaster impact, and thus social and economic vulnerability are critical components. Vulnerability maps are very useful in identifying areas at potentially high risk of flooding and to better understand the determinants of vulnerability in order to identify planning and capacity building needs, or to better target funding and adaptation/mitigation programs (de Sherbinin, 2014). However, few efforts have been made to standardize vulnerability measurement and estimation techniques. This is true particularly in developing countries and for non-economic measures (Wright, 2015). In the context of flood risk management, the sensibility of a community refers to the degree to which that community is affected or responsive to the flooding, while the adaptive capacity defines the potential or capability of a community to adapt to (to alter to better suit) to the flooding or their effects or impacts (Ipcc, 2007). One of the common approaches to quantify flood vulnerability and

risk is to construct an index by combining various indicators (Yoon, 2012). This is the approach used in the assessment of the vulnerability of Malanville in this research. The selection of indicators that best describe the adaptive capacity and the sensibility of the communities at risk in the research district was guided by the literature review on factors known to affect both components as well as data availability and quality (Chai-onn, 2015). Data availability is one of the major factors that influences the selection of the indicators (Tapsell *et al.*, 2010). The socio-economic indicators used in this study are derived from Benin 2013 General Census of Population and Housing (INSAE, 2016).

To describe the adaptive capacity of the study area, information such as the number of health centers and the access to drinking water were selected as indicators.

The sensibility in the area of interest was assessed by building indicators from data such as the percentage of women in the communities, the percentage of old and young in the population and the ratio of agricultural population in the exposed communities. Land use/cover is another critical factor of the flood vulnerability that needs to be accounted for. Thereby, each type of land use was ranked relating to their susceptibility to flooding.

Figure 4.7: sensitivity and adaptive capacity indicator

Vulnerability Component	Indicator	Measurement	influence of the indicator on the vulnerability
Sensitivity	Gender	Proportion of women in the population.	-
	Agricultural population	Proportion of the population whose livelihood depends on agriculture	-
	Age < 5	rate of the population under 5 years old	-
	Age > 60	rate of the population over 60 years of age	-
Adaptive capacity	Access to drinking water	Proportion of Household that has access to drinking water	+
	Health	Number of health infrastructure in the district	+

Baseline assessment using the data available from the Benin 2013 General Census of Population and Housing(INSAE, 2015).

The variables considered in this study were measured in different units. To be able to aggregate these variables and create a composite score of vulnerability, a standardization procedure was applied. The development of the different indicators was undertaken using a Min-Max scaling transformation. In this standardization technique, the values of the indicators are rescale between zero and one, with 0 being the worst rank for the considered indicator and 1 being the best (Yoon, 2012). One advantage of this approach is that separate maps for each vulnerability component (e.g., into exposure, sensitivity and adaptive capacity) can help decision-makers to analyze adaptation options (Nardo, et al, 2014)

The vulnerability indicators are normalized as follows:

$$X_i' = \frac{X_i - MIN(X_i)}{MAX(X_i) - MIN(X_i)} \quad \text{Equation 9}$$

Where:

$$X_i' = Normalized\ value\ of\ Sensitivity/Adaptive\ \ indicator$$

$$X_i = Observed\ Value\ of\ Sensitivity/Adaptive\ indicator$$

$$MIN(X_i) = Minimum\ observed\ value$$

$$MAX(X_i) = Maximum\ Observed\ value$$

The adaptive capacity variable and the vulnerability has an inverse relationship, in other words, a high adaptive capacity is associated with a low vulnerability. Thus, prior to averaging the vulnerability indicators, the following formula was applied to the adaptive capacity indicator:

$$X_i'' = 1 - X_i' \quad \text{Equation 10}$$

Where: X_1'' is the new adaptive capacity score.

The total vulnerability index of the district was obtained by computing the arithmetic mean of the standardized vulnerability indicator values (sensitivity, adaptive capacity and land use) at the level of each district. No weighting factor was applied on the indicators because like in most vulnerability studies, the indicators here, are considered independent and equally important (Yoon, 2012). The final vulnerability index ranges between 0 and 1.

4.2.6 Flood Risk Assessment

Risk is the result of the interplay between hazard and vulnerability (Dewan, 2013). Although there is no single definition of risk (Klijn *et al.*, 2009), it is often considered as the product of the hazard and vulnerability (Wisner *et al.*, 2005). This concept of risk has been the base of the evaluation of the flood risk in the study area. Following the stimulation of the different flood scenarios, the flood depths were normalized on a range between 0 and 1. This was done in order to adjust the flood depth on a common scale with the vulnerability indicators. Using the field calculator tool, available in the ArcGIS toolbox, the product of the total vulnerability and the normalized flood depth was spatially computed to generate the flood risk map.

Risk = hazard × vulnerability Equation 11

CHAPTER 5

5. RESULT AND DISCUSSION

5.1 Flood frequency analysis

The analysis of the flood frequency is a crucial step in the evaluation of the hazard. The frequency analysis was performed on both the Niger River and the Sota River (a tributary of the Niger River) discharge data.

5.1.1 Niger River discharge frequency analysis

The Figure 5.1 presents the simulated maximum annual discharge by the HYPE model of the SMHI on the Niger River between 1980 and 2009.

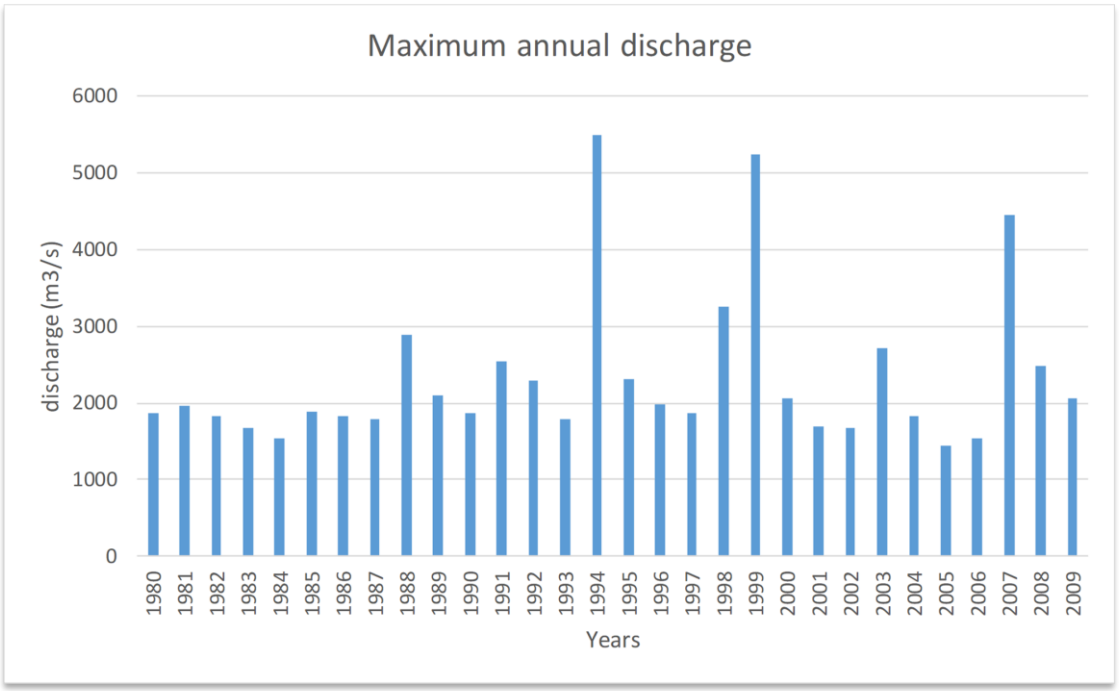

Figure 5.1: Maximum annual discharge Niger River

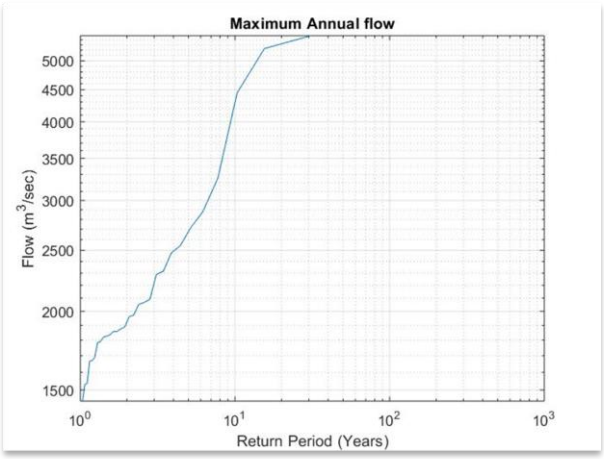

Figure 5.3: return period

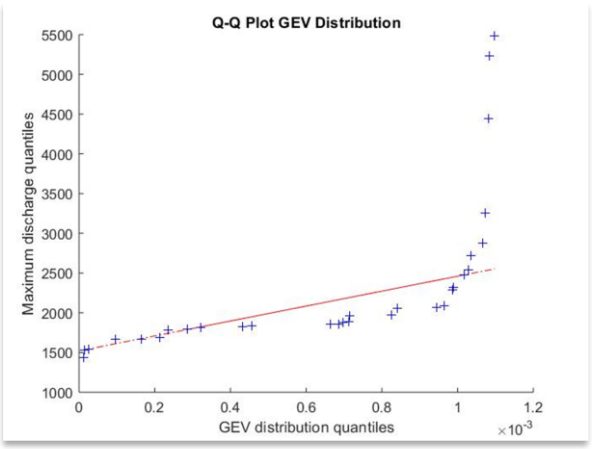

Figure 5.2: Q-Q plot (GEV)

After fitting several probability distributions on the set of data, the goodness of fit was assessed through the Quantile-Quantile plot statistical test. The Q-Q plotting between the flow data and the theoretical values of the Generalized Extreme Value distribution does not fall about a straight-line (figure 5.5). However, from the Q-Q plotting between the maximum annual discharge data and the Gumbel distribution, both grow at the same pace between the discharge quantile of approximately 1300 m^3/s and 3200 m^3/s; therefore their quantile match in this region. However, looking at the Q-Q plot, if the flow data followed the Gumbel distribution, the last two maximum annual discharges should be inferior to 4500 m^3/s, when in fact those quantiles are greater than 5000 m^3/s. This is due to the occurrence of floods with a large return period within the 30 years period river flow dataset.

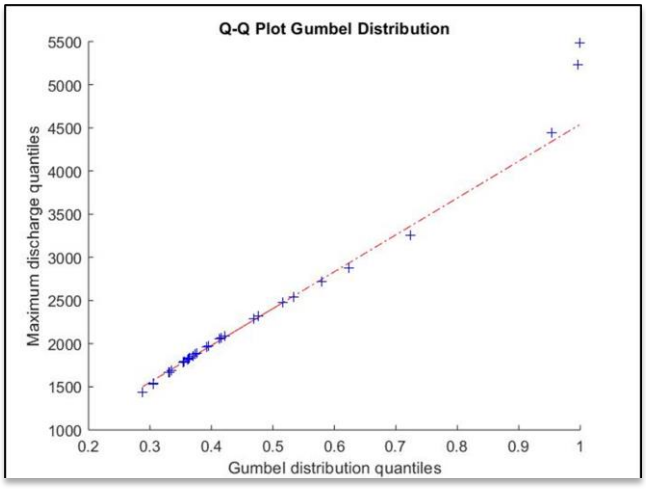

Figure 5.4: QQ-plot (Gumbel)

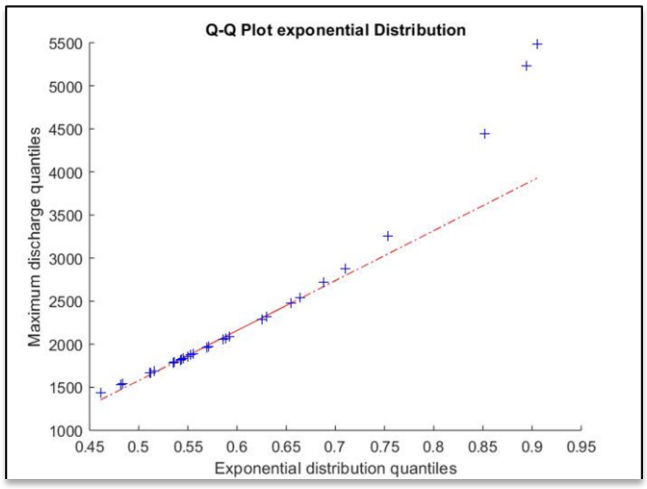

Figure 5.5 QQ-plot (Exponential)

Nevertheless, there was a better fit with the Gumbel distribution than with the other fitted distribution. Thus, the extrapolation of the different return period used in this study was performed using the Gumbel distribution. Table 5.1 presents the result of the extrapolation.

Table 5.1: designed flood (Niger)

Return Period	10 years	20 years	50 years	80 years	100 years
Maximum discharge (m^3/s)	4051	4410	4774	4929	4997

5.1.2 Sota River discharge frequency analysis

The figure 5.6 presents the maximum annual discharge of the Sota River between 1980 and 2009. The Quantile-Quantile plotting between the Gumbel distribution and the Sota river discharge (Figure 5.7) revealed only one outlier which shows a good fit between the maximum annual discharge data and the Gumbel distribution.

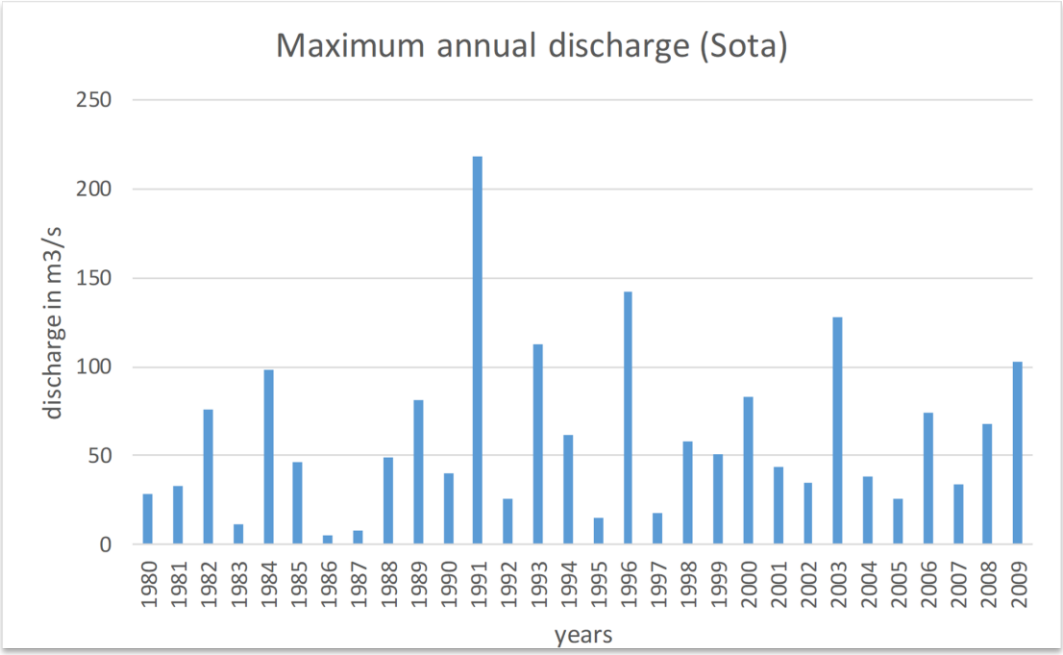

Figure 5.6: maximum annual discharge (Sota river)

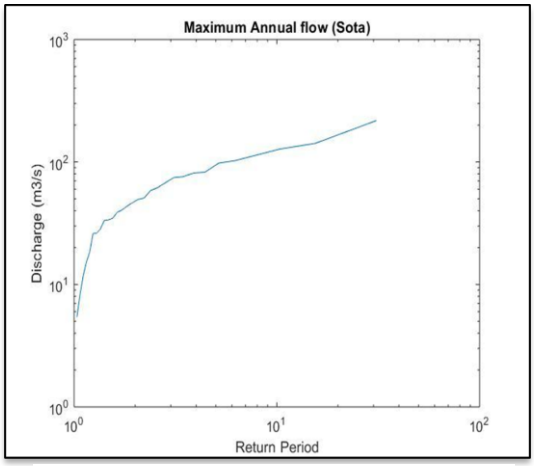

Figure 5.8: Return period (Sota)

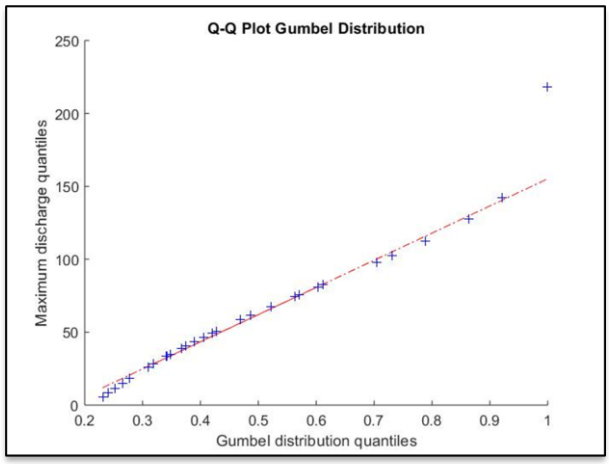

Figure 5.7: Q-Q plot (Gumbel distribution)

The table 5.2 presents the discharge corresponding to the 10 years, 20 years, 50 years, 80 years, and 100 years return period flood.

Table 5.2: designed flood (Sota)

Return period	10 years	20 years	50 years	80 years	100 years
Discharge (m3/s)1	136	152	168	175	178

5.2 River geometry

Overall, 100 cross-sections were drawn to describe the geometry of the main river and 234 cross-sections were generated for the tributary (La Sota). The cross section N° 28444.87 was used as the upstream boundary conditions. While the cross-section N° 642,669 of the main river was used to set the downstream boundary conditions.

5.3 Land use/Land Cover Map

The land use maps of the study area were prepared by performing a supervised classification of a Landsat 8 image of Malanville captured on the 17 April 2018. A signature file was generated by analyzing existing land use maps of the study area and information gathered from Google Earth. Afterwards, the area of interest was classified into five different land uses types: built-up area, cultivated floodplain, water bodies, forest and bare soil. The table shows the different land use types and the occupied area. As it is shown in the Table 5.3 cultivated floodplain (61%) and forest (23%) are the most common land use types found in the study area. A little more than 4% of the total area of the District of Malanville is built up.

Table 5.3: land use/ land cover classification

Land use type	Area in km^2	Proportion of total area %
Water	6.61	3.61
Cultivated floodplain	112.82	61.63
built-up area	7.80	4.26
Forest	42.33	23.12
Bare soil	13.50	7.37

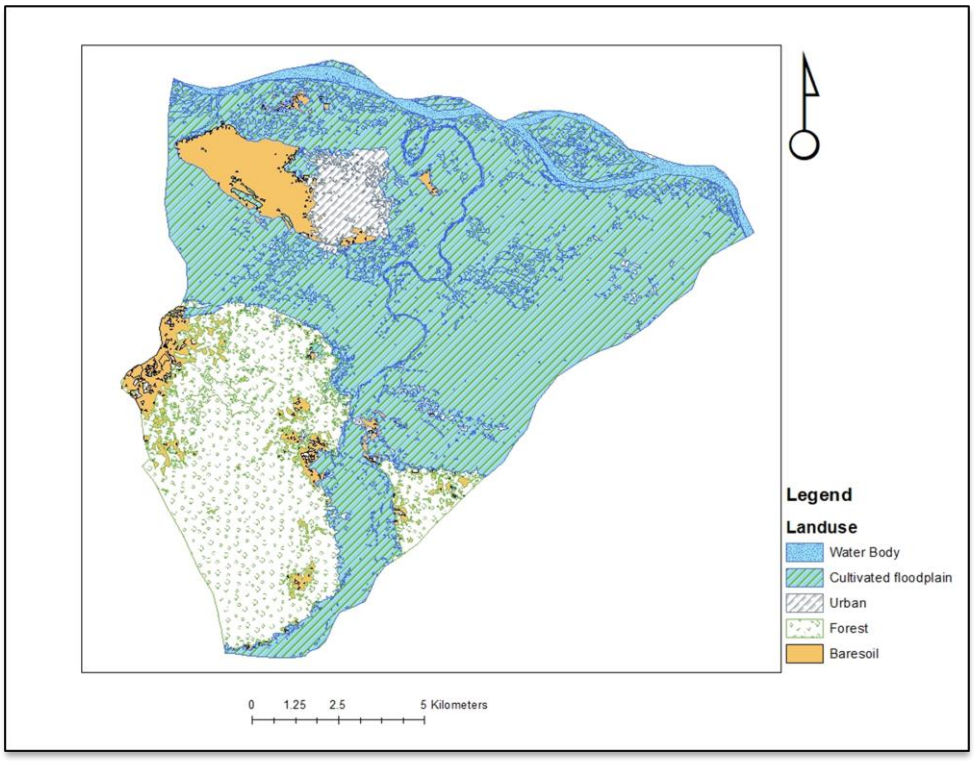

Figure 5.9: Land use/ Land cover map of the district of Malanville

Figure 5.10: Satellite image of bare soil Malanville (source: google earth)

Figure 5.11: Satellite image of built-up area, Malanville (source: google earth)

Figure 5.13: Satellite image of floodplain, Malanville (source: google earth)

Figure 5.12: Satellite image of forest, Malanville (source: google earth)

5.4 Friction Coefficient and Model Calibration

The calibration of the model was performed on the Manning friction coefficient using as starting point the reference values given by Chow (1959). After the classification of the different land use types in the area of interest, each of them was assigned a Manning n coefficient. During the calibration process of the model, the friction coefficient was varied and the mapped flood extents were compared with the flooded area captured by a Landsat 8 image (4 September 2013) of the historical flood of September 2013. The discharge data of the flood of 2013 were obtained from the Niger Basin Authority.

Figure 5.14: Landsat 8 image flood extent (2013)

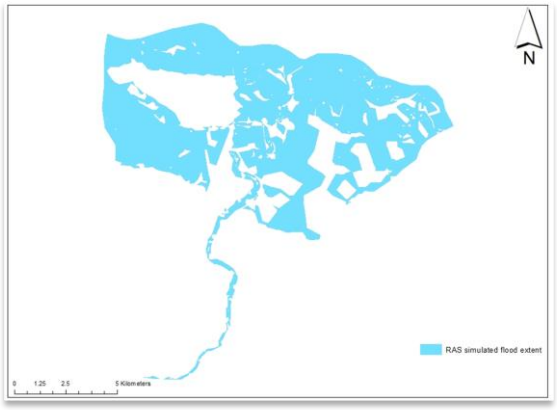

Figure 5.15: RAS simulated flood extent (2013)

The Table 5.4 presents the different land use types with their associated Manning coefficients before and after calibration.

Table 5.4: Manning' n coefficient value before and after calibration

Land use type	Manning' n value before calibration	Manning after calibration
Main channel	0.07	0.085
cultivated floodplain	0.035	0.05
Urban	0.02	0.035
Forest	0.1	0.115
Bare soil	0.030	0.045

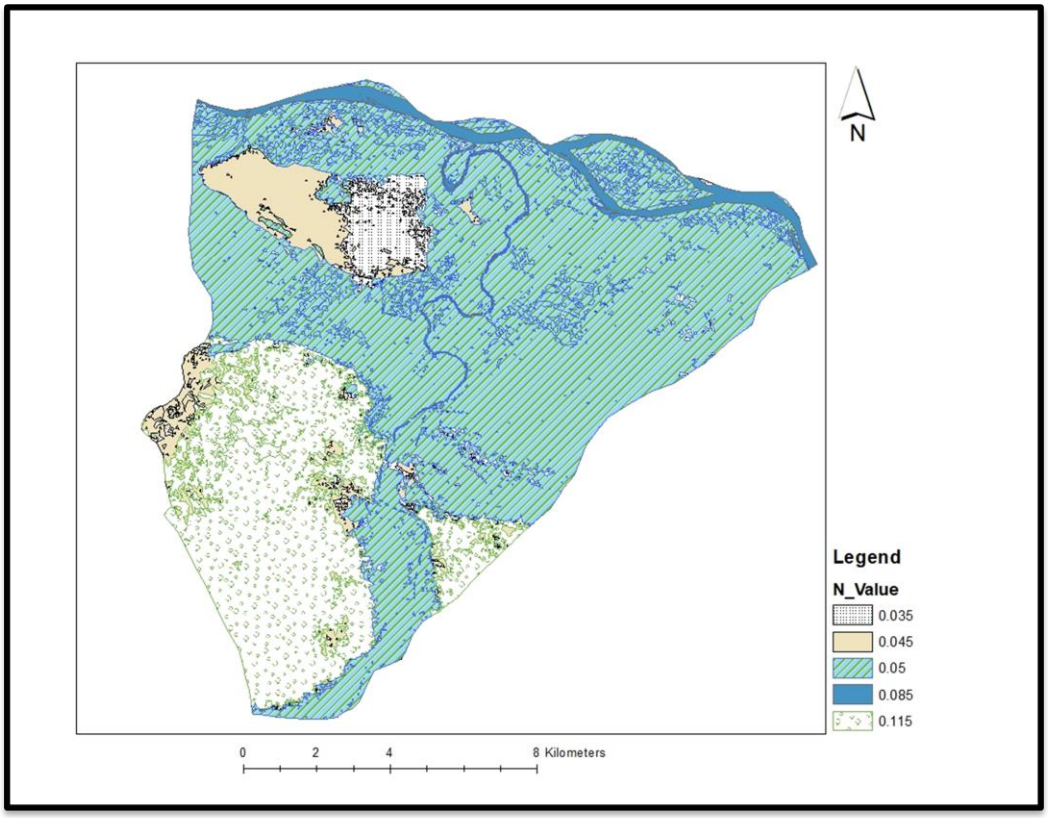

Figure 5.16: friction coefficient map

5.5 Validation

The model was validated by using information from the historical flood of September 2017. A Landsat 8 image (15 September 2017) of the flood extent was compared to the inundated area computed by the hydrodynamic model. The observed flood extent area is 66.01 km^2 while the simulated one is 76.36 km^2. There was an overestimation of 13.55% of the flooded area by the model. The overestimation of the flood extent is explained by the low resolution of the DEM being unable to capture accurately the river morphology and the error in the selection of the friction coefficient. Furthermore, the presence of a dike, built to protect irrigated rice fields in Malanville was not accounted for in the flood modeling with HEC-RAS which could also explain the overestimation of the flood extent by the model.

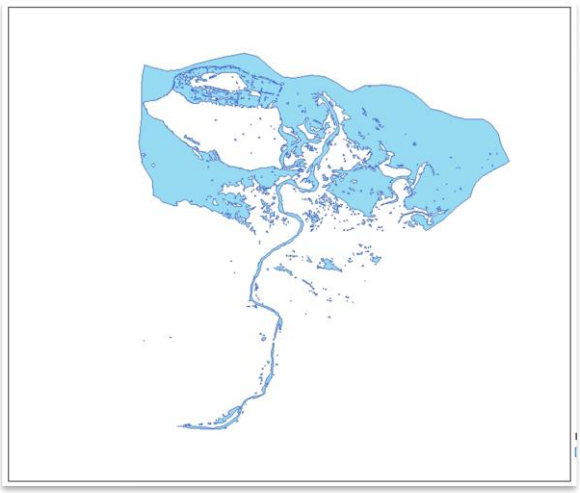

Figure 5.18: Landsat 8 image flood extent (2017)

Figure 5.17: HEC-RAS simulated flood extent (2017)

The Table 5.5 shows the flooded area by land use type for the simulated and the observed. From the results, there has been an overestimation of the water extent in the floodplain and in the built-up area by the model, while the flooded bare soil and forest areas were underestimated.

Table 5.5: simulated and observed flooded area for each land use type

Land use type	Flooded area km^2 (Simulated)	Flooded area km^2 (Observed)
Water	6.31	6.54
Cultivated floodplain	67.73	58.61
Urban	0.8	0.73
Forest	0.07	0.014
Bare soil	1.30	0.06

5.6 Results of the Hydrodynamic Modelling and Exposure Assessment

The output of the simulation was in the form of water depth and water extent at each cross-section location. Once exported to ArcGIS, this information was mapped by using the HEC-GeoRAS extension in ArcMap. The generated maps show clearly the inundated area and the variation of the water depth for each selected return period. Flood hazard maps are the main tools for flood control and flood management studies (NRC, 2009). The goal of the flood hazard map is to display information about the probability and the magnitude of a flood event, e.g. Flood extent and water depth distribution. Once the flood hazard map is overlaid on a

land-use map, it becomes possible to identify the assets and the communities that are exposed to the different return period floods.

5.6.1 10-year return period flood

Figure 5.19 shows the water extent and the water depth for the 10 years return period floods in the district of Malanville and the table 5.6 presents the classification of the land use type by the simulated flood depth for the same return period.

In the scenario of a 10 years return period flood, 47.26% of the area of the district of Malanville will be inundated and 88.6% of the affected areas are part of the cultivated floodplains areas. Furthermore, about 16.5% of the inundated area in the district will be subjected to a water depth higher than 3m and most of this area (81%) is located in the floodplain. While 16% of the built-up area will be flooded in the 10 years recurrence interval scenario, less than 19% of this area will be affected by a water depth higher than 3 m.

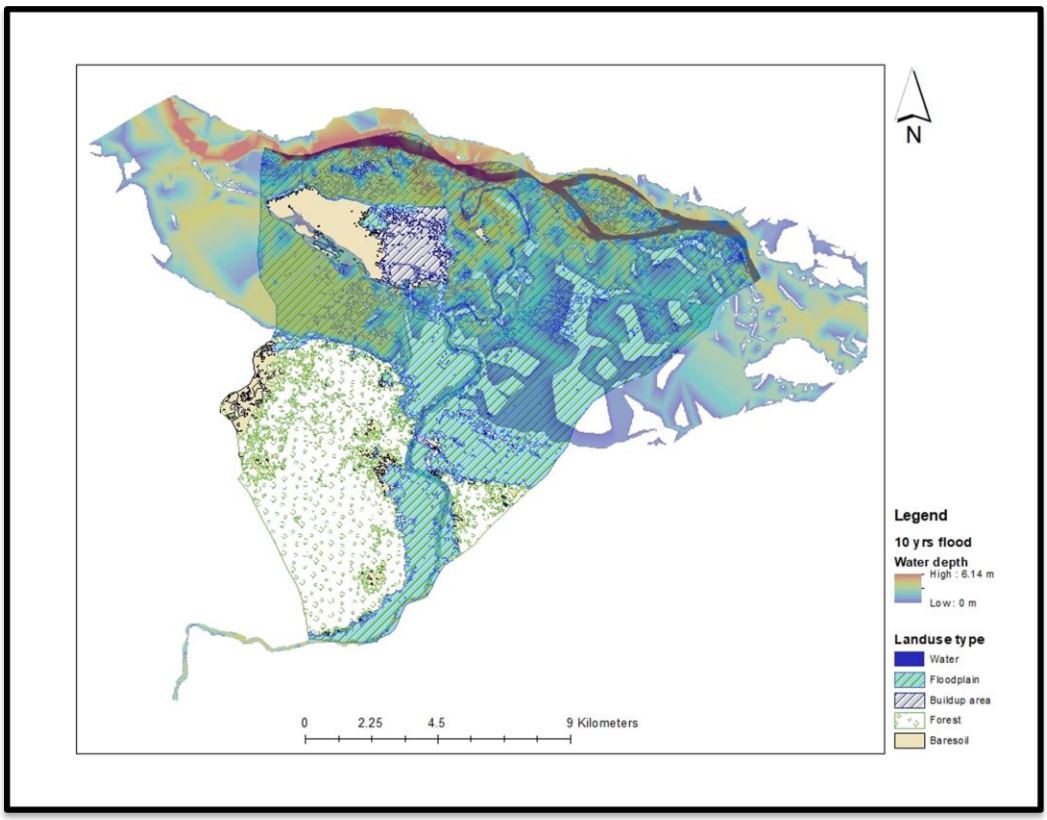

Figure 5.19: 10 years return period flood map

Table 5.6: land use distribution by simulated flood depth for the 10yrs return period flood

Depth/Land Use	water	floodplain	Built-up area	Forest	Bare soil	Total
0-1	0.21	18.18	0.54	0.08	0.81	19.82
1-2	0.37	19.57	0.34	0.06	0.69	21.03
2-3	0.77	14.14	0.15	0.02	0.33	15.41
3-4	1.56	21.13	0.21	0.00	0.10	23.01
4-5	1.97	3.33	0.02	0.00	0.00	5.32
5-6	1.56	0.38	0.00	0.00	0.00	1.95
Total	6.44	76.74	1.26	0.15	1.94	86.53

5.6.2 20 years recurrence interval flood

Figure 5.20 presents the flood map (depth and extent of the flood) in the case of the 20 years return period flood. A classification of the flood depth according to the land use type is presented in the Table 5.7. Roughly, 48.10% of the area of Malanville will be submerged by the flood of 20 years recurrence interval, and 1.51% of the affected areas are built-up. As it is the case with the 10 years return period flood, most of the affected area (88.6%) is located in the floodplain. When analyzing the water depth, it appears that 63.7% of the flooded area will be under a water depth lower than 3 m.

Table 5.7: land use distribution by simulated flood depth for the 20yrs return period flood

Depth/Land Use	water	floodplain	Built-up	Forest	Bare soil	total
0-1	0.20	17.45	0.57	0.08	0.82	19.12
1-2	0.34	19.07	0.34	0.06	0.73	20.53
2-3	0.74	15.17	0.17	0.02	0.37	16.47
3-4	1.38	21.90	0.22	0.00	0.13	23.63
4-5	2.09	4.00	0.03	0.00	0.00	6.12
5-6	1.70	0.48	0.00	0.00	0.00	2.18
Total	6.46	78.07	1.33	0.16	2.05	88.06

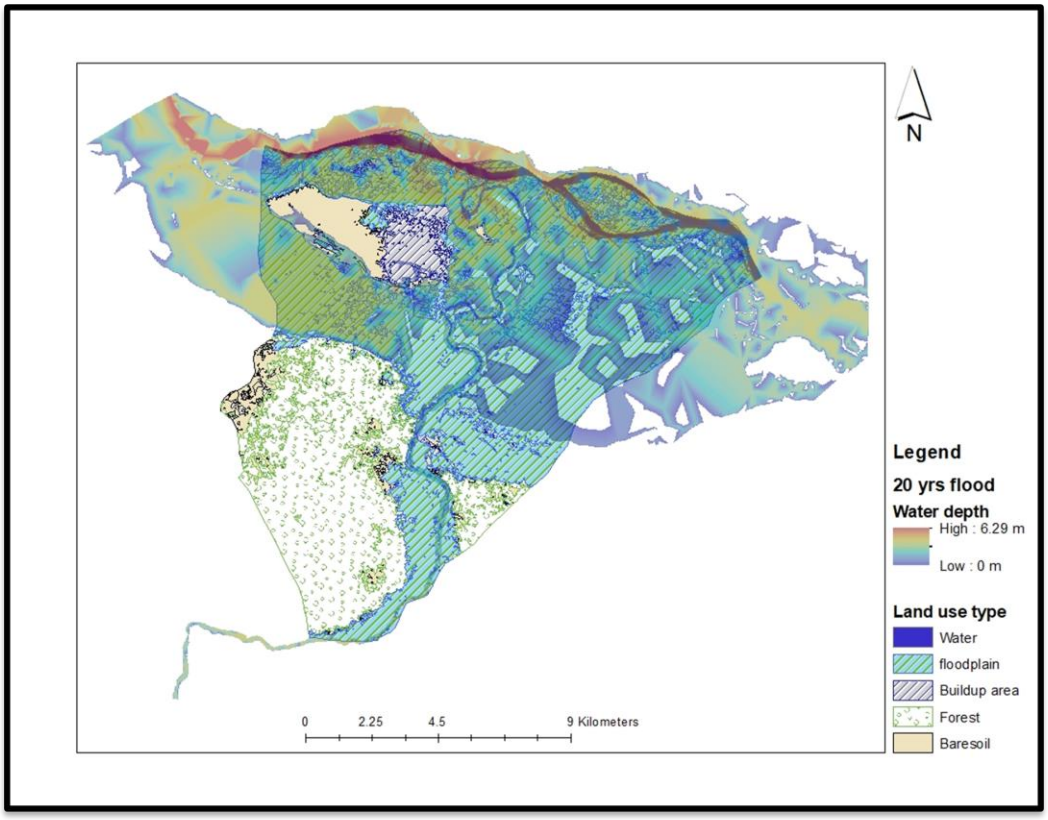

Figure 5.20: 20 years return period flood map

5.6.3 50 Years Return Period Flood

The result of the simulation of the 50 years return period flood scenario is presented in the Figure 5.21 and the Table 5.8. The flood of 50 years recurrence intervals would lead to a flooded area of approximately 89.5 Km^2, which represents 48.8 % of the total area of the district. 1.6 % of the total-affected areas of the district are built-up areas. As for the water level, compared to the 20 years return period floods, more land will be subjected to water depth higher than 3 m in the 50 years return period floods. Indeed while 36.3 % of the inundated area in the 20 years return period flood scenarios was under a water depth higher than 3 m, this increased to 37.46% in the 50 years return period flood scenario. However, in both cases the majority of the affected areas by a water depth higher than 3 m are located in the floodplains. This was also the case in the 10 years return period flood scenario.

Table 5.8: land use distribution by simulated flood depth for the 50yrs return period flood

Depth/Landuse	water	floodplain	Built-up	Forest	Bare soil	total
0-1	0.18	15.56	0.60	0.08	0.84	17.26
1-2	0.33	19.80	0.33	0.06	0.73	21.25
2-3	0.69	16.12	0.18	0.02	0.44	17.45
3-4	1.31	22.09	0.24	0.00	0.14	23.77
4-5	2.15	5.15	0.04	0.00	0.02	7.36
5-6	1.80	0.59	0.00	0.00	0.00	2.39
6-7	0.01	0.00	0.00	0.00	0.00	0.01
total	6.47	79.30	1.40	0.17	2.16	89.50

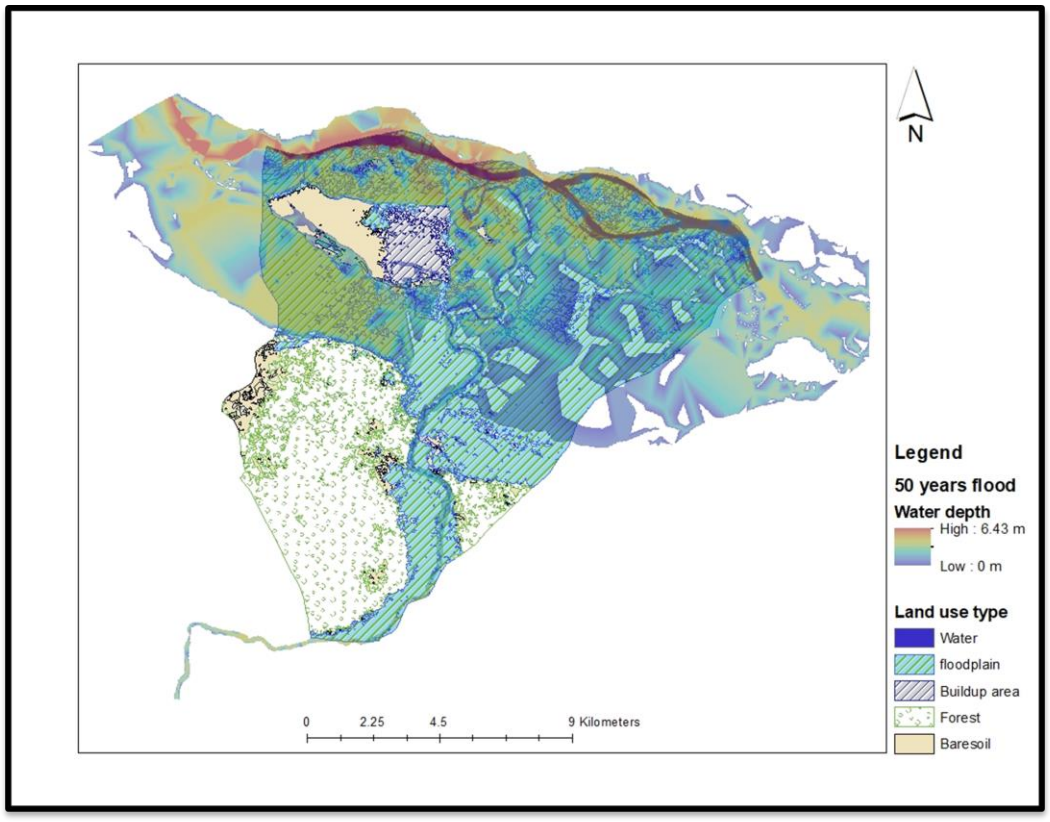

Figure 5.21: 50 years return period flood map

5.6.4 80 years return period flood scenario

Table 5.9 and Figure 5.22 present the result of the simulation of the flood of 80 years recurrence intervals. The result of the hydrodynamic modelling shows that 49% of the land of the district of Malanville is flooded in the case of the 80 years return period flood. Compared to the 50 years return period flood, there is an increase of 1.59% of the flooded area. The built-up land accounts for 1.6% of the total inundated area in the event of the 80 years return period flood which represents 18% of the total built-up area. There is not much of an increase of the flooded built-up areas compared to the 50 years return period flood scenario. The analysis of the water depth in general shows that more land are exposed to higher water level than in the 50 years return period flood scenario. None of the built-up areas will be affected by a water level higher than 6m during the flood event.

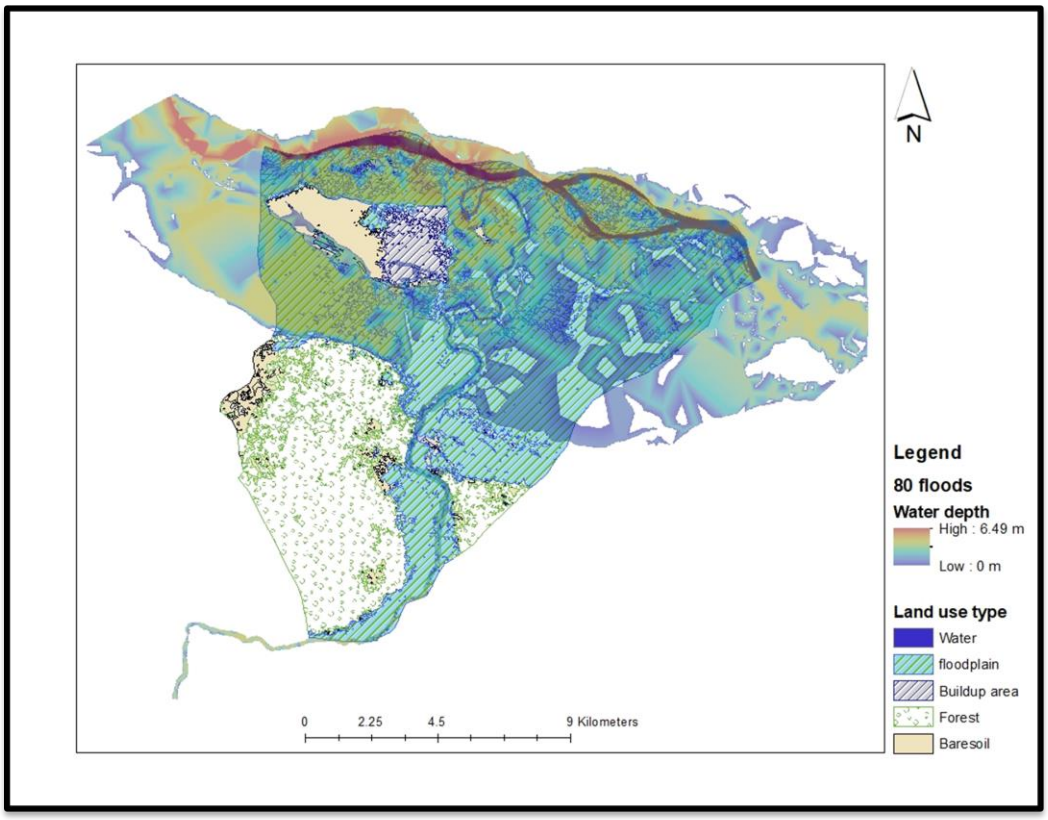

Figure 5.22: 80 years return period flood map

Table 5.9: land use distribution by simulated flood depth for the 50yrs return period flood

Depth/Landuse	water	floodplain	Built-up	Forest	Bare soil	Total
0-1	0.18	15.23	0.62	0.08	0.83	16.93
1-2	0.32	19.74	0.34	0.07	0.75	21.22
2-3	0.66	16.36	0.19	0.03	0.46	17.69
3-4	1.28	22.19	0.24	0.00	0.14	23.85
4-5	2.18	5.57	0.05	0.00	0.02	7.82
5-6	1.77	0.63	0.00	0.00	0.00	2.41
6-7	0.08	0.00	0.00	0.00	0.00	0.08
Total	6.47	79.73	1.43	0.17	2.19	90.00

5.6.5 100 years return period flood

The highest recurrence interval that was considered in this study in the flood hazard analysis was the 100 years return period. The results of the simulation are shown in the Table 5.10 and the Figures 5.23. During a 100 years flood scenario, 90.26 km^2 of the area of Malanville would be underwater; this represents 49.3% of the total area of the district. Furthermore, it is only in the 100 years return period flood that it was noticed a water level higher than 6m in the built-up area.

Table 5.10: land use distribution by simulated flood depth for the 100yrs return period flood

Depth/Land Use	water	floodplain	Urban	Forest	Bare Soil	total
0-1	0.18	15.05	0.62	0.08	0.82	16.74
1-2	0.32	19.76	0.34	0.07	0.72	21.21
2-3	0.65	16.47	0.19	0.03	0.50	17.85
3-4	1.25	19.29	0.24	0.00	0.14	20.92
4-5	2.20	8.73	0.06	0.00	0.02	11.01
5-6	1.64	0.66	0.00	0.00	0.00	2.30
6-7	0.23	0.00	0.00	0.00	0.00	0.23
Total	6.47	79.95	1.45	0.18	2.21	90.26

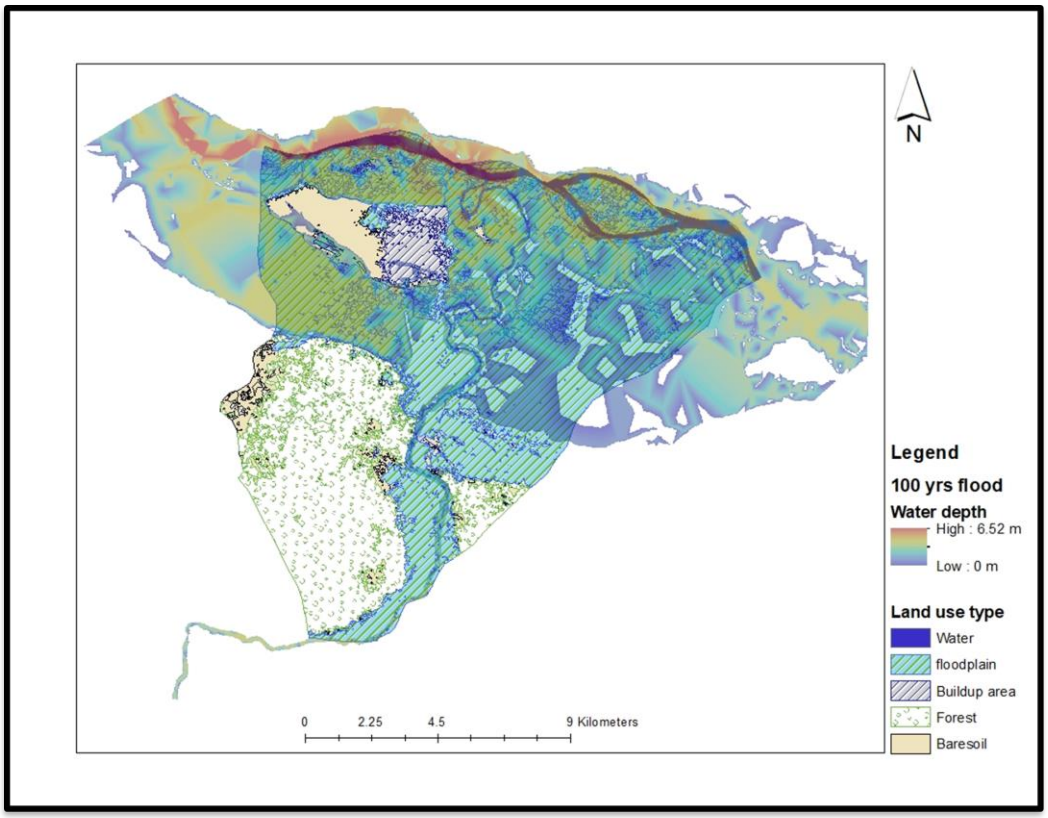

Figure 5.23: 100 years return period flood map

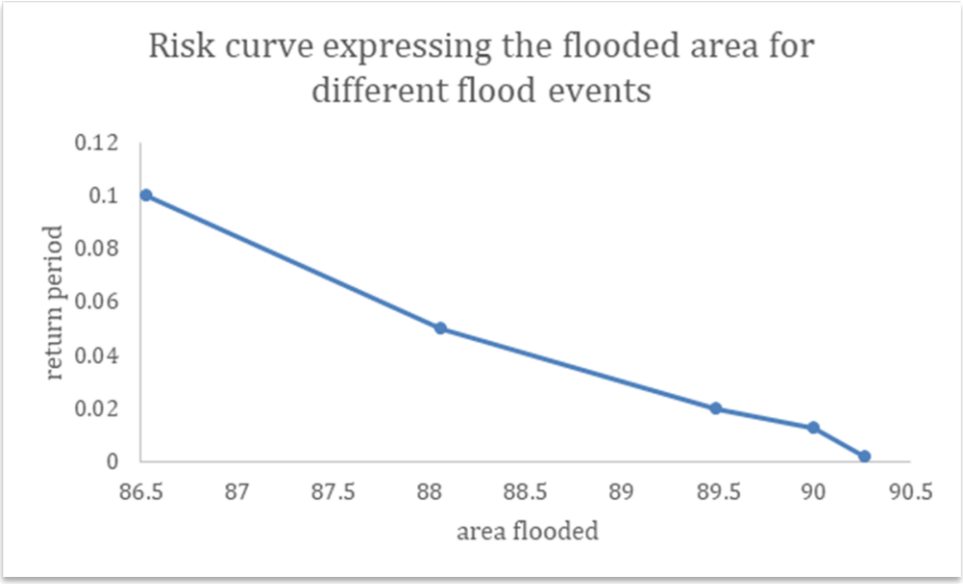

Figure 5.24: Risk curve for area flooded for different return

5.7 Results of the Vulnerability assessment

Population distribution

The Table 5.11 presents the population distribution in each township of the district of Malanville. Tassi-Tedji and Wollo are the two most populated township while Tassi-Zenon is the least populated.

Table 5.11: Population distribution in the district of Malanville (INSAE, 2016)

District	Population	Percentage %
MOMKASSA	4031	6
BODJECALI	7597	11
GALIEL	9401	14
KOKI	4137	6
TASSI TEDJI	22661	33
TASSI ZENON	2715	4
WOLLO	13562	20
WOURO-HESSO	4566	7
Total	68670	100

5.7.1 Land use and vulnerability

In order to prepare the vulnerability map, each land use type was ranked between 0 and 4 by considering the assets present on the land. Therefore, the built-up areas were given the highest-ranking number while the water and the bare soil have the lowest. Subsequently the land use ranks were standardized on a scale between 0 and 1, with 1 implying a high vulnerability of the land use types and 0 a low vulnerability. The vulnerability scores of each land use type are summarized in the Table 5.12 below.

Table 5.12: Land use vulnerability score

Land use type	Water	Flood plain	Urban	Forest	Bare soil
Rank	0	3	4	2	0
Normalized vulnerability scores	0	0.75	1	0.5	0

5.7.2 Adaptive capacity, sensitivity and vulnerability

Figure 5.25 presents the results of the analysis of the sensitivity and the adaptive capacity in the district of Malanville using the indicator based method. It should be noted that the values of the indicators have been standardized on a scale between 0 and 1. Figure 5.25 indicated that the most vulnerable townships of Malanville are Bodjecali and Wouro-hesso; both indeed have a high sensitivity and a low adaptive capacity. This trend can be observed, in the high proportion of old and young people in the population as well as the low proportion of households with access to drinking water and the lack of health centers in both township. On the contrary, Tassi Tedji, Galiel and Tassi Zenon are the least vulnerable. The relatively low agricultural population, the high rate of households with access to drinking water and the availability of health centers are some indicators of the low vulnerability of these townships.

Table 5.13: sensitivity indicators (source INSAE)

Indicators/ Districts	BODJECALI	GALIEL	KOKI	TASSITEDJI	TASSIZENON	WOLLO	WOURO-HESSO	MOMKASSA
percent females (PFEMALES)	0.5	0.48	0.52	0.51	0.51	0.5	0.51	0.51
percent agricultural population (PAGRICULT)	0.76	0.36	0.94	0.13	0.17	0.39	0.1	0.83
percent population under 5 years (PAGE5YRS)	0.24	0.22	0.26	0.2	0.17	0.23	0.2	0.23
percent population over 60 years (PAGE60YR)	0.03	0.04	0.03	0.03	0.05	0.04	0.05	0.04

Table 5.14: Normalized sensitivity indicators

Districts	PFEMALES	PAGRICULT	PAGE5YRS	PAGE60YR	Sensitivity score
BODJECALI	0.57	0.78	0.80	0.19	0.59
GALIEL	0.00	0.31	0.57	0.29	0.29
KOKI	1.00	1.00	1.00	0.00	0.75
TASSITEDJI	0.65	0.04	0.36	0.05	0.27
TASSIZENON	0.72	0.09	0.00	1.00	0.45
WOLLO	0.51	0.34	0.64	0.31	0.45
WOURO-HESSO	0.79	0.00	0.36	1.00	0.54
MOMKASSA	0.77	0.87	0.65	0.28	0.64

Table 5.15: Adaptive capacity indicators

Indicator/District	BODJECALI	GALIEL	KOKI	TASSI-TEDJI	TASSI-ZENON	WOLLO	WOURO-HESSO	MOMKASSA
Percent households with access to safe drinking water (PHWASDW)	24.7	33.8	67.8	40.4	74.8	33.5	34.3	74.5
Number of Health center (NHEALTHC)	0	1	1	1	1	0	0	0

Table 5.16: Normalized adaptive capacity indicators

Districts	BODJECALI	GALIEL	KOKI	TASSI - TEDJI	TASSI - ZENON	WOLLO	WOURO-HESSO	MOMKASSA
PHWASDW	1	0.82	0.14	0.69	0	0.82	0.81	0.01
NHEALTHC	1	0	0	0	0	1	1	1
adaptive capacity score	1	0.41	0.07	0.34	0	0.91	0.9	0.5

In the estimation of the total vulnerability of the study area, each element (physical, social, and existing coping capacity attributes) upon which the vulnerability depends were taken into consideration. By using the standard deviation from the mean, the vulnerability index values were classified as either very low, low, moderate, high or very high.

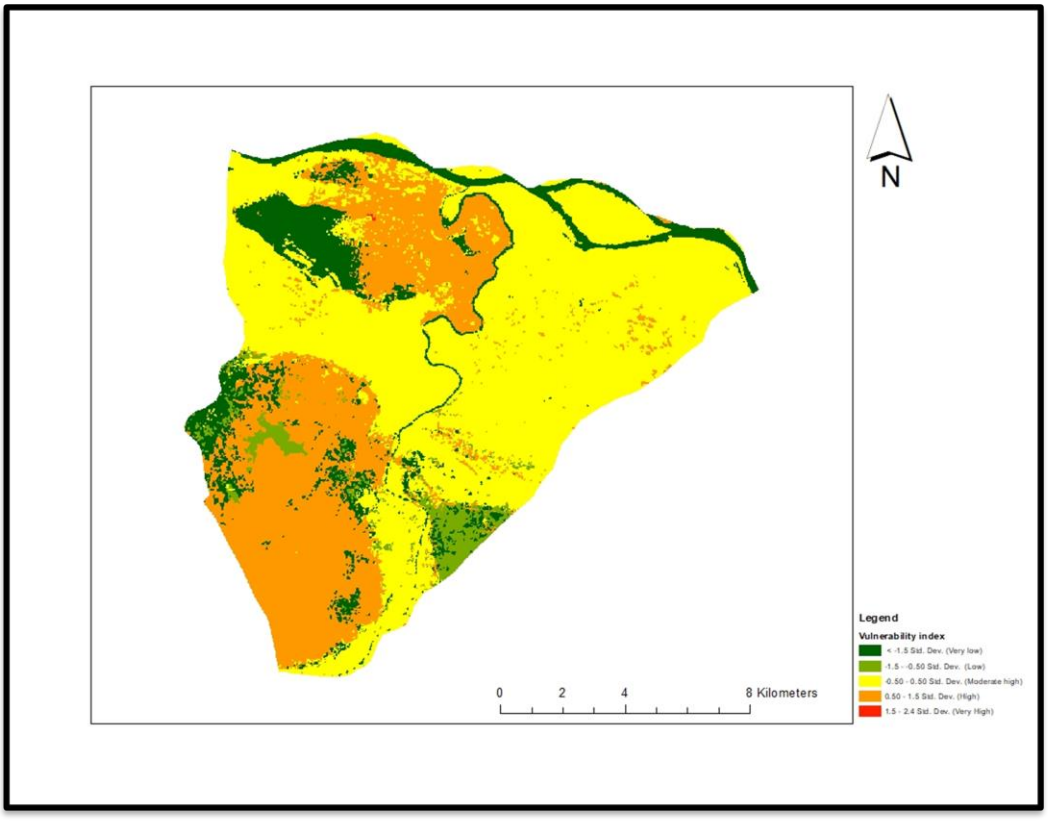

Figure 5.25: vulnerability map (Adaptive capacity, sensitivity and land use type)

5.8 Flood risk assessment

Flood risk maps are essential for the flood management planning. In the mapping of the flood risk, both the vulnerability and the flood hazard were considered. Risk is the product of vulnerability and hazard. The classification of the risk index was performed by using their quantiles. Table 5.17 presents the classification of the risk score with regards to the quantiles.

Table 5.17: Risk classification

Risk score (Quantile)	Risk
0.000	Very low
0.00 - 0.103	Moderate
0.103 - 0.213	High
0.213 - 0.472	Very high

Table 5.18 presents the different levels of flood risk in terms of affected total area in the district of Malanville for each considered flood scenario. The proportion of the area at a very low risk of inundation for the different floods scenarios varies between 54.4% and 56.4%, while for a very high risk the percent of the area-concerned lies between 15% and 17%. A high proportion of the cultivated floodplain is at high or very high risk of flooding in all the considered scenarios. Bearing in mind that most of the floodplain areas are cultivated by a high proportion (37%) of the population of Malanville district, the flood poses a high risk to their livelihood and to the food security in the district.

Table 5.18: Summary of total area by level of flood risk

Return period / Risk	10 years	% 10 years	20 years	% 20 years	50 years	% 50 years	80 years	% 80 years	100 years	% 100 years
Very Low	103.8	56.4	102.1	55.5	100.8	54.8	100.4	54.6	100.2	54.4
Moderate	21.4	11.6	20.2	11.0	18.4	10.0	18.2	9.9	18.0	9.8
High	31.3	17.0	32.5	17.7	34.1	18.5	34.3	18.6	34.4	18.7
Very high	27.6	15.0	29.3	15.9	30.7	16.7	31.1	16.9	31.5	17.1
Total	184.1	100.0	184.1	100.0	184.1	100.0	184.1	100.0	184.1	100.0

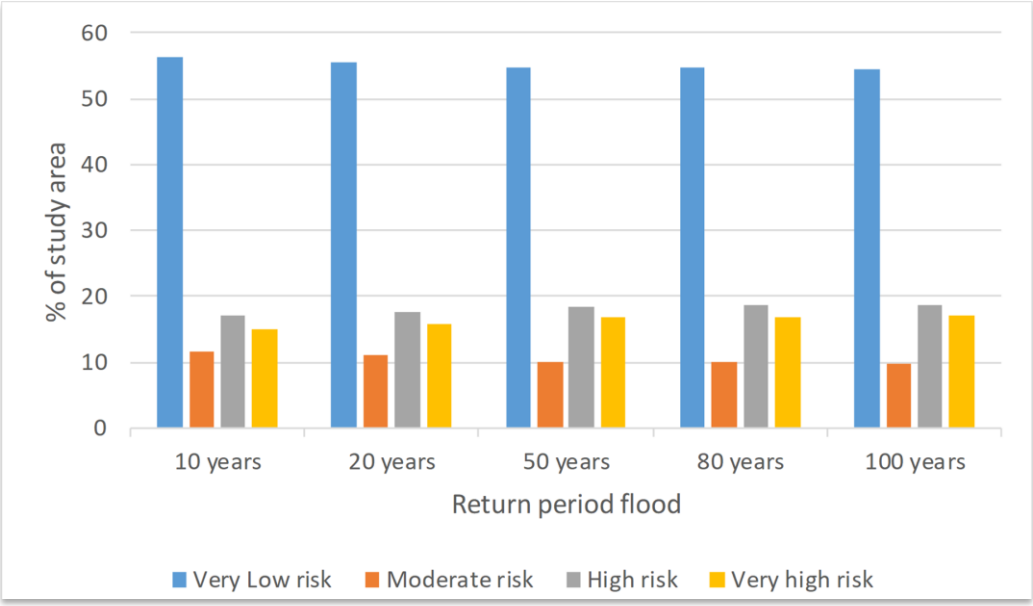

Figure 5.26: Affected area by flood risk level

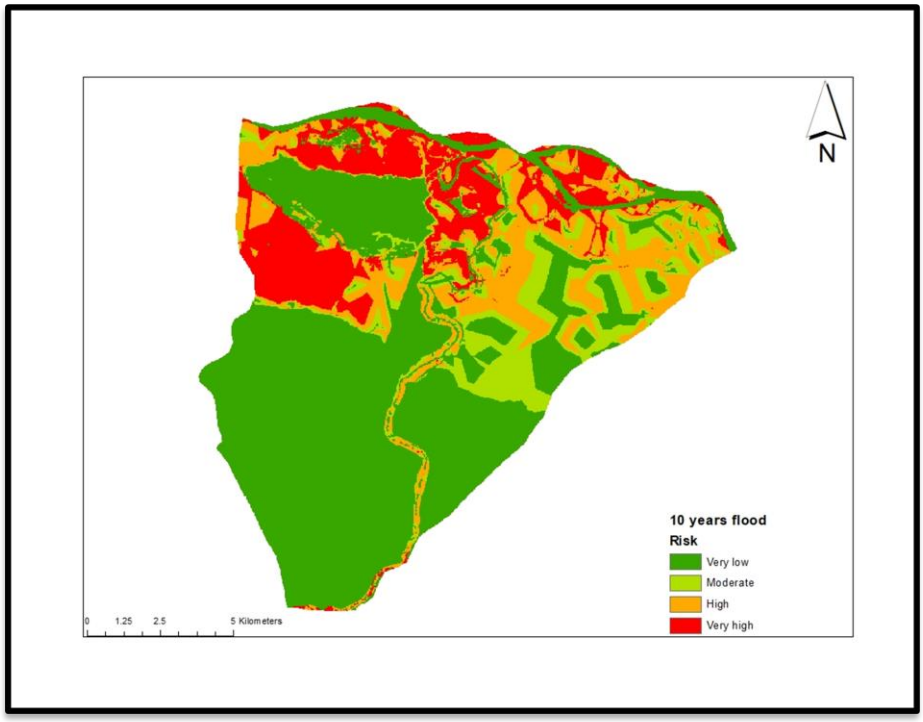

Figure 5.27: Flood risk map (10 years return period)

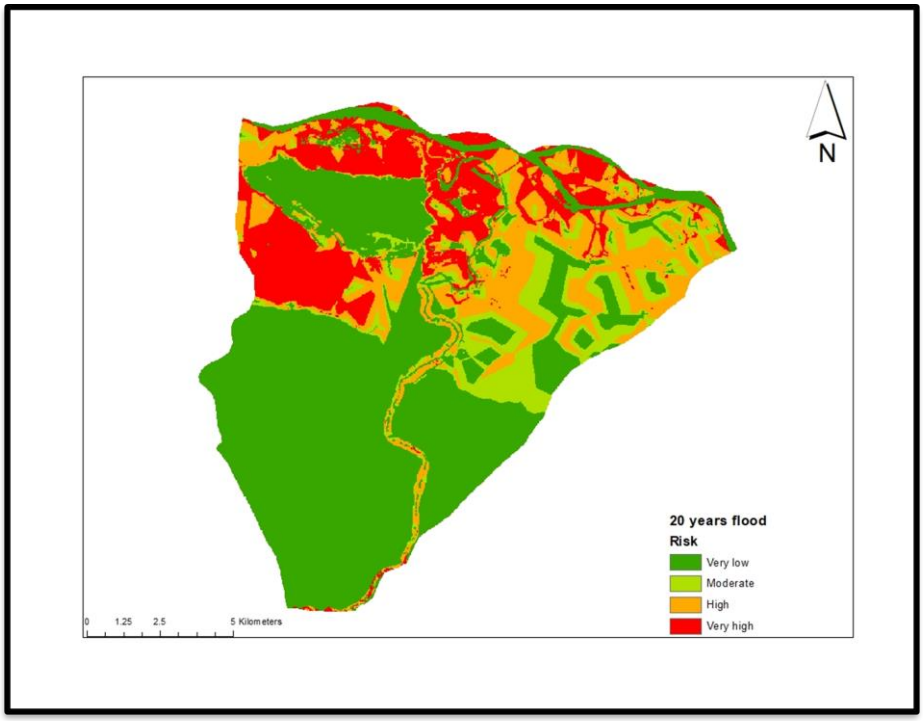

Figure 5.28: Flood risk map (20 years return period)

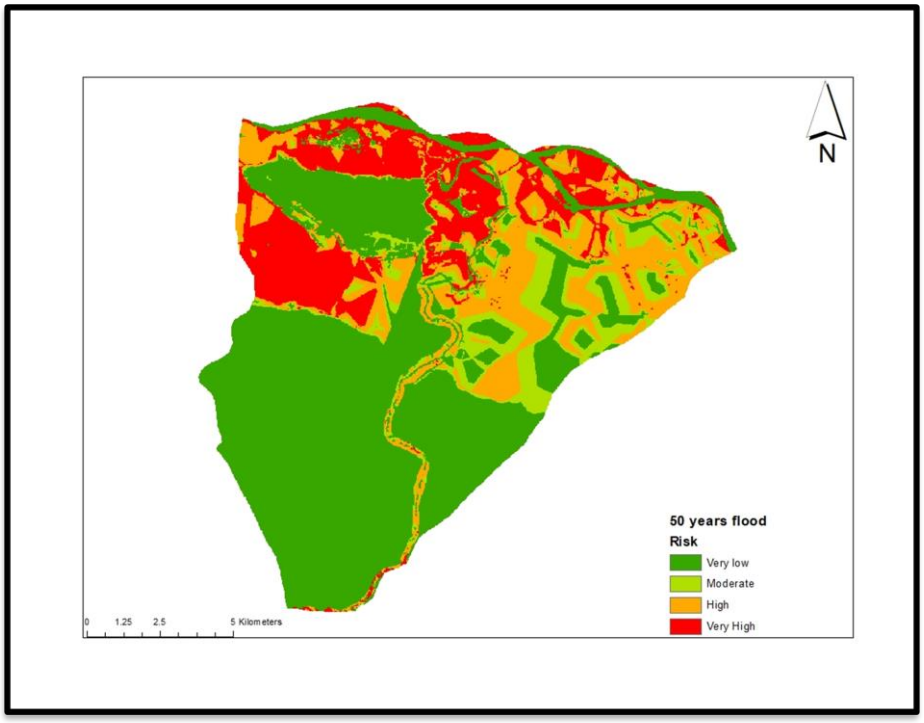

Figure 5.29: Flood risk map (50 years return period)

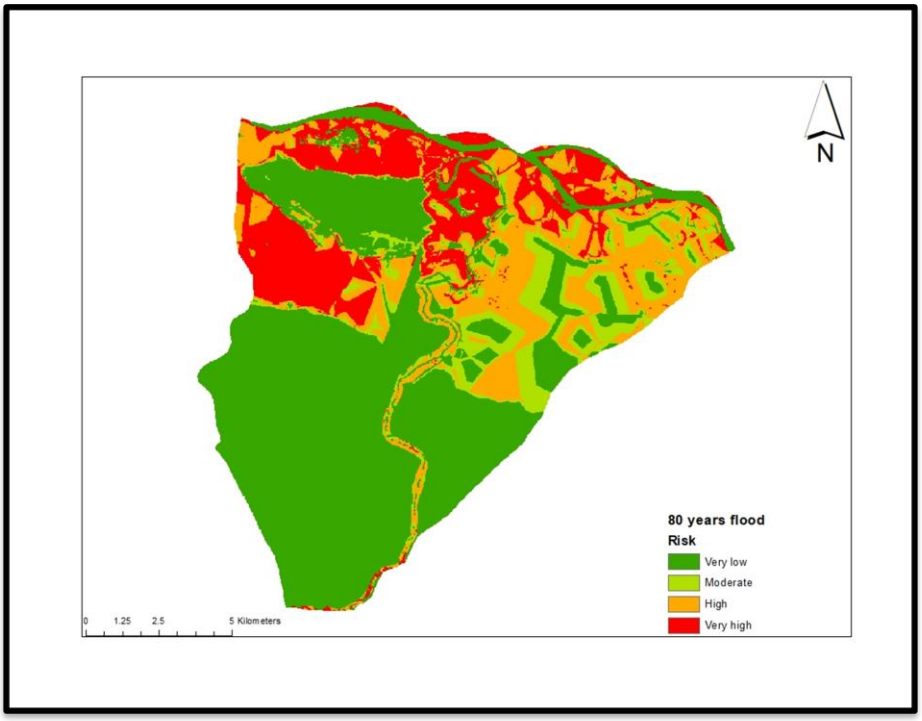

Figure 5.30: Flood risk map (80 years return period)

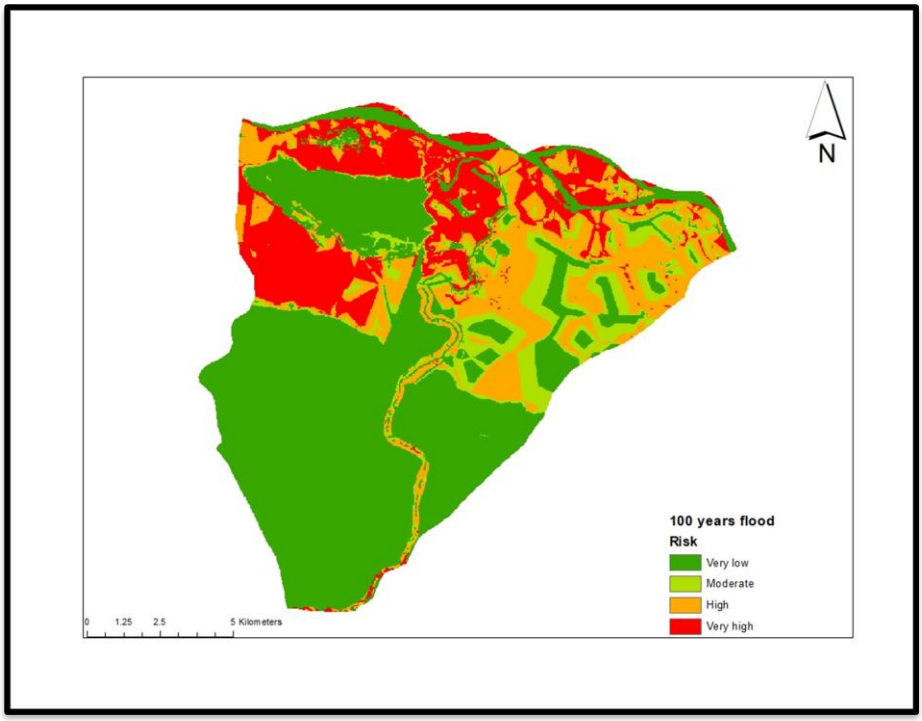

Figure 5.31: Flood risk map (100 years return period)

Table 5.19: Malanville' townships flood risk

Township/Flood scenario	10yrs	20yrs	50yrs	80yrs	100yrs
MOMKASSA	High risk	High risk	High risk	High risk	High risk
BODJECALI	Very low risk	Very low risk	Very low risk	Very low risk	Very low risk
GALIEL	Very High risk	Very High risk	Very High risk	Very High risk	Very High risk
KOKI	Very low risk	Very low risk	Very low risk	Very low risk	Very low risk
TASSI TEDJI	Very low risk	Very low risk	Very low risk	Very low risk	Very low risk
TASSI ZENON	Very low risk	Very low risk	Very low risk	Very low risk	Very low risk
WOLLO	Very low risk	Very low risk	Very low risk	Very low risk	Very low risk

5.9 General discussion

The annual flooding of the Niger River puts a strain on the economy of the region. This is particularly true for the District of Malanville located on the right bank of the Niger River. An understanding of the causality of the flood risk in the Niger River Basin could assist decision-makers in the implementation of an appropriate flood risk management plan. The goal of the present study was to assess the flood risk in the district of Malanville using geospatial technics and hydrodynamic modelling. Over the past decade, more than seven flood events have been recorded in Malanville (https://www.emdat.be/). These flood events have affected the lives and the livelihood of the different communities of the district. The analysis of the flood hazard was performed with the hydraulic model HEC-RAS. Both the floods probabilities and their magnitudes were taken into consideration in the assessment.

From the result of the hydrodynamic modelling it was found that between 47% and 50% of the study area will be flooded during the different flood scenarios (10 yrs, 20 yrs, 50 yrs, 80 yrs, and 100 yrs) simulated. However, the water depth exceeds 6m only in the case of the flood of 50 yrs, 80 yrs and 100 yrs return period. Before the risk assessment, an evaluation of the vulnerability of the communities at risk was conducted in order to acquire knowledge about the sensitivity to floods and the adaptive capacity of the different communities in the study area. Identifying communities that are vulnerable to natural hazards can significantly contribute to disaster risk reduction (Tan *et al.*, 2012). The analysis has revealed that the townships of Bodjecali and Wouro-Hesso are the most vulnerable to the flooding. However, because these townships are not exposed to the hazard, there are located in a low-risk zone of flooding. The township most at risk of flooding are Momkassa and Galiel. Indeed, the flood risk assessment revealed that in every flood scenario studied, Momkassa and Galiel are located in a high-risk zone and in a very high-risk zone, respectively. This is related to their high vulnerability and exposure to high water level during the floods. A little less than 20% of the population of the district of Malanville dwell in the townships of Momkassa and Galiel. Thereby, it is paramount to implement measures to alleviate the flood risk to the population of both townships. This can be done by raising their adaptive capacity through the building of more health centers in the townships and the increasing of their access to potable water. Likewise, it is important to raise the awareness of the populations of the townships on the risk they are facing. Communities play a significant role in flood risk management, thus the necessity of involving them at each stage of the decision-making process regarding the flood risk management.

Moreover, the highest proportion of land use types located in a zone of high or very high risk are the cultivated areas along the Niger River and the Sota River. This situation pose a challenge to the food security in the area of interest and to the livelihood of the population. Indeed, a high proportion (37%) of the population of Malanville are farmers, and most of their cultivated lands are located in the floodplains.

In fact, one of the most important consequences associated to previous flood events in the area of interest has been the loss of agricultural production.

CHAPTER 6

6. Conclusions and recommendations

6.1 Conclusions

The Niger is a transboundary river located in West Africa; it is the third-longest river in Africa, exceeded only by the Nile and the Congo River, it floods annually causing material damage and most alarming the loss of human lives. Studies have shown an increase of the frequency and the magnitude of floods in the NRB over the decades (Geo, 2015). Even though extreme events cannot be prevented, a better understanding of the risk pose by such events is the first stage in building the resilience of the community. The analysis of the risk associated with flooding produces knowledge about the hazard and the vulnerability of the population at risk.

This thesis was carried out to assess the flood risk in the district of Malanville located along the Niger River. In order to analyze the flood hazard a hydrodynamic model (HEC-RAS) was set up for the study area and different flood scenarios were simulated. As for the vulnerability, each of its components were analyzed by using an indicator-based approach. The results from the flood hazard assessment and the vulnerability analysis were combined to produce a flood risk map of the study area.

- The use of a hydrodynamic model provided an objective way to model flooding. Given that, this approach considers the spatial variability of river characteristics such as the friction coefficient and the riverbed geometry. However, the modelling was faced with a lack of data in the study area namely topographic data and discharge data on the Niger River and its tributary. Thus, the use of simulated and remotely sensed data in the different analyses was performed.
- Through GIS techniques, hydraulic modelling results can be presented in a more publically intelligible manner and can provide exploitable knowledge for the decision makers in the flood risk management planning process.
- The assessment of the flood hazard revealed that only a small proportion (between 1.26% and 1.43%) of the built-area in the district would be flooded in the different flood scenarios considered. The most flooded areas of the districts are the floodplains. This situation poses a threat to the economy of the region given that a high proportion of the population grows crops in these floodplains for their livelihood.
- The study of the vulnerability of the area of interest was performed by analysing each of its components (exposure, adaptive capacity, sensitivity) with the indicator-based approach. This technique is simple and easy to implement in a GIS and the results are useful for comparing the spatial variability of vulnerability across different spatial units (Connelly et al, 2015). From the analysis, it was discovered that the townships of Bodjecali and Wouro-Hesso are the most

vulnerable of the district due to the lack of health infrastructure and a high proportion of the most vulnerable sections of society in their population.

- By combining the flood analysis and the vulnerability assessment results, the study evaluated the flood risk in the district. Two townships of the district of Malanville are at high and very high risk of flooding, while the other townships are located in areas of low risk. Monkassa and Galiel, the two townships at high and very high risk of flooding, respectively are not only vulnerable to the floods but also exposed to high levels of water during the different simulated flood scenarios. In order to minimize the effects of the disasters in both townships, it is imperative to respond appropriately to reduce their vulnerability. This could be done by raising awareness in the communities and through a better land use planning. Furthermore, the implementation of a people-centered early warning system could help manage the disaster in the district. An EWS people centered is comprised of the four following element: (1) knowledge of the risks; (2) monitoring, analysis and forecasting of the hazards; (3) communication or dissemination of alerts and warnings; (4)and local capabilities to respond to the warnings received (UN, 2006).
- The overall purpose of this thesis was to produce sufficient knowledge to elaborate a flood risk management plan that provides the adequate adaptation/mitigation measures to alleviate the threat posed by the hazard to the different communities of the District of Malanville.

6.2 Recommendations

Throughout the course of this study, data availability was a major constraint. This situation required the use of alternative sources of data, namely global dataset that are not always adapted to the different analysis that were carried out.

- This study used a low resolution (30 m) Digital Elevation Model (DEM) in the assessment of the flood hazard. It is recommended for future research to perform field survey measurement of the river bathymetry in order to build a more accurate river morphology.
- Using a 30 years record to extrapolate the 100 years return period floods can raise the level of uncertainty in the results. Therefore, it will be important to look into the extent of errors related to the extrapolation. Likewise, with climate change in play relying solely on historical data to simulate the future is bound to carry a great deal of uncertainty. Hence, this study recommended taking into consideration the climate change aspects in studies such as flood risk assessment.
- One of the weaknesses of the indicator-based vulnerability assessment approach used in this research is the non-consideration of the interdependency amongst the variables. We recommend to apply a regression analysis in order to study the relationship between the different indicators.

Reference

Ackerman, P. E. C. T. (2011) 'HEC-GeoRAS GIS Tools for Support of HEC-RAS using ArcGIS ® User â€™ s Manual', (February), p. 244.

Adewale, P. O., Sangodoyin, A. Y., & A. (2011) 'Flood routing in the Ogunpa River in nigeria', *The Electronic Journal of the International Association for Environmental Hydrology*, 19(October), pp. 1–15.

Aich, V. *et al.* (2014) 'Floods in the Niger basin – analysis and attribution', *Natural Hazards and Earth System Sciences Discussions*, 2(8), pp. 5171–5212. doi: 10.5194/nhessd-2-5171-2014.

Aich, V. *et al.* (2016) 'Time series analysis of floods across the Niger River Basin', *Water (Switzerland)*, 8(4). doi: 10.3390/w8040165.

Behanzin, I. D. *et al.* (2016) 'GIS-Based Mapping of Flood Vulnerability and Risk in the Bénin Niger River Valley', 6(3).

Chai-onn, T. (2015) 'Hotspots Mapping : Implementing the Spatial Index Approach', (November).

Chow, V. Te (1959) 'Open Channel Hydraulics', *Open Channel Hydraulics*. doi: 10.1016/B978-0-7506-6857-6.X5000-0.

Connelly, A., Carter, J. and Handley, J. (2015) 'State of the Art Report (4) Vulnerability Assessment', (4).

Dewan, A. (2013) *Floods in a Megacity: Geospatial Techniques in Assessing Hazards, Risk and Vulnerability*. doi: 10.1007/978-94-007-5875-9.

Eleuterio, J. (2012) 'Flood risk analysis : impact of uncertainty in hazard modelling and vulnerability assessments', p. 243pp.

Forkuo, E. K. (2013) 'the Use of Digital Elevation Models for Water- Shed and Flood Hazard Mapping', *International Journal of Remote Sensing & Geoscience*, 2(2), pp. 56–65. Available at: www.ijrsg.com.

Geo, U. (2015) 'Floods in the Niger River Basin in the face of Global Change Analysis , Attribution and Projections'.

GWP (2007) 'APPLYING ENVIRONMENTAL ASSESSMENT FOR FLOOD MANAGEMENT A Tool for Integrated Flood Management', (March 2007).

Hicks, F. E. and Peacock, T. (2005) 'Suitability of HEC-RAS for Flood Forecasting', *Canadian Water Resources Journal*, 30(2), pp. 159–174. doi: 10.4296/cwrj3002159.

INSAE (2015) 'Rgph4 : Que Retenir Des Effectifs De Population En 2013 ?', *République du Bénin*, p. 35.

INSAE (2016) 'Cahier des villages et quartiers de ville Département de l'Alibori', p. 17. Available at: file:///C:/Users/Roland/Downloads/ATLANTIQUE.pdf.

Ipcc (2007) *Climate Change 2007: impacts, adaptation and vulnerability: contribution of Working Group II to the fourth assessment report of the Intergovernmental Panel, Genebra, Suíça*. doi: 10.1256/004316502320517344.

Józsa, E., Fábián, S. Á. and Kovács, M. (2014) 'An evaluation of EU-DEM in comparison with ASTER GDEM, SRTM and contour-based DEMs over the Eastern Mecsek Mountains', *Hungarian Geographical Bulletin*, 63(4), pp. 401–423. doi: 10.15201/hungeobull.63.4.3.

Kai, G., Monica, R. Della and Mampuya, H. (2004) 'Building Disaster Resilience To Natural Hazards in

Sub-Saharan African Regions, Countries and Communities'. Available at: http://www.unisdr.org/files/55070_55070acpeuprogrammebrochurefinal.pdf.

Kaplan, S. *et al.* (1981) 'On The Quantitative Definition of Risk', *Risk Analysis*, 1(1), pp. 11–27. doi: 10.1111/j.1539-6924.1981.tb01350.x.

Khaleghi, S., Mahmoodi, M. and Karimzadeh, S. (2015) 'Integrated application of HEC-RAS and GIS and RS for flood risk assessment in Lighvan Chai River', *International Journal of Engineering Science Invention*, 4(4), pp. 38–45.

Klijn, F. *et al.* (2009) 'Flood risk assessment and flood risk management: An introduction and guidance based on experiences and findings of FLOODsite - Report Number T29-09-01', *FLOODsite Deltares, Delft Hydraulics, Delft, the Netherlands*, p. 143. doi: 978 90 814067 1 0.

Koutsoyiannis, D. (2004) 'Statistics of extremes and estimation of extreme rainfall: I. Theoretical investigation', *Hydrological Sciences Journal*, 49(4), pp. 575–590. doi: 10.1623/hysj.49.4.575.54430.

Mai, D. and De Smedt, F. (2017) 'A Combined Hydrological and Hydraulic Model for Flood Prediction in Vietnam Applied to the Huong River Basin as a Test Case Study', *Water*, 9(11), p. 879. doi: 10.3390/w9110879.

Martini, F. and Loat, R. (2007) 'Handbook on good practices for flood mapping in Europe', *European exchange circle on flood mapping*, p. 60. doi: 10.1016/j.cageo.2011.11.027.

MESSNER, F. and MEYER, V. (2005) 'Flood Damage, Vulnerability and Risk Perception – Challenges for Flood Damage Research', *Flood Risk Management: Hazards, Vulnerability and Mitigation Measures*, pp. 149–167. doi: 10.1007/978-1-4020-4598-1_13.

Mukolwe, M. M. (2016) *Flood Hazard Mapping Uncertainty and its Value in the Decision-making Process*. doi: ISBN 978-1-138-03286-6.

Nardo, M., Saisana, M., Saltelli, A., Tarantola, S., Hoffman, A., A. and Giovannini, E. (2014) 'Spatial Climate Change Vulnerability Assessments : a Review of Data , Methods , and Issues', (August), pp. 1–70. doi: 10.13140/2.1.1888.0002.

Pistrika, a and Tsakiris, G. (2007) 'Flood risk assessment: A methodological framework', *Water Resources Management: New …*, (June), pp. 14–16. Available at: http://www.ntua.gr/hazard/publications/EWRA_2007.Pistrika.pdf.

Pitt, M. (2008) 'The Pitt Review: Learning Lessons from the 2007 Floods', *Floods Review*, p. 19,. doi: 10.1007/s13398-014-0173-7.2.

Sayers, P. *et al.* (2013) *Flood Risk Management: A Strategic Approach, Water and Sewerage Journal*. Available at: http://www.sayersandpartners.co.uk/uploads/6/2/0/9/6209349/flood-risk-management-web.pdf.

de Sherbinin, A. M. (2014) 'Mapping the unmeasurable? Spatial Analysis of Vulnerability to Climate Change and Climate Variability', (August), p. 234. doi: 10.3990/1.9789036538091.

Tan, B. *et al.* (2012) 'Determinants of Risk : Exposure and Vulnerability Coordinating Lead Authors : Lead Authors : Review Editors : Contributing Authors ':, pp. 65–108.

Tapsell, S. *et al.* (2010) 'Social vulnerability to natural hazards', *Contract*, 1(11), p. 524. Available at: http://caphaz-net.org/outcomes-results/CapHaz-Net_WP4_Social-Vulnerability2.pdf.

Thieken, A. and Merz, B. (2006) 'Methods for flood risk assessment: concepts and challenges', *International Workshop on Flash Floods in Urban Areas*, (May 2016). Available at:

http://www.researchgate.net/profile/Heiko_Apel/publication/228677524_Methods_for_flood_risk_assessment_Concepts_and_challenges/links/02e7e51c1a4f7c8817000000.pdf.

Timbadiya, P. V., Patel, P. L. and Porey, P. D. (2011) 'Calibration of HEC-RAS Model on Prediction of Flood for Lower Tapi River, India', *Journal of Water Resource and Protection*, 3(11), pp. 805–811. doi: 10.4236/jwarp.2011.311090.

Udani, P. M. and Mathur, D. K. (2016) 'Flood hazard vulnerability mapping using remote sensing & GIS : A case study along the villages of Anand taluka', 7(3), pp. 214–221.

UN (2006) 'Global Survey of Early Warning Systems', *An assessment of capacities, gaps and opportunities toward building a comprehensive global early warning system for all natural hazards*, p. 56. Available at: http://www.unisdr.org/ppew/info-resources/ewc3/Global-Survey-of-Early-Warning-Systems.pdf.

UNEP (2002) 'United Nations Environment Programme- UNEP in 2002. Nairobi, Kenya. UNT Digital Library. http://digital.library.unt.edu/ark:/67531/metadc25989/.', *Development*. Available at: http://www.unep.org/gc/gc22/Media/UNEP_Annual_Report_2002.pdf.

UNISDR (2009) '2009 UNISDR Terminology on Disaster Risk Reduction', *International Stratergy for Disaster Reduction (ISDR)*, pp. 1–30. doi: 978-600-6937-11-3.

UNISDR (2016) 'Disaster Risk Reduction in Africa, Status Report - 2015, Executive summary', pp. 1–7. doi: 10.1002/aehe.3640230702.

USACE (2016) 'HEC-RAS River Analysis System - Hydraulic Reference Manual, Version 5.0', (February), p. 547. doi: CPD-68.

Wisner, B. *et al.* (2005) 'At Risk: Natural Hazards, People's Vulnerability, and Disasters', *Journal of Homeland Security and Emergency Management*, 2(2). doi: 10.2202/1547-7355.1131.

Wright, D. B. (2015) 'Methods in Flood Hazard and Risk Assessment', pp. 1–20.

Yoon, D. K. (2012) 'Assessment of social vulnerability to natural disasters: A comparative study', *Natural Hazards*, 63(2), pp. 823–843. doi: 10.1007/s11069-012-0189-2.

Annex

1. Measured Daily discharge (m3/s) of the Niger River at Malanville for the year 2013 (source ABN GIRE2/NIGER-HYCOS - SIH/HIS)

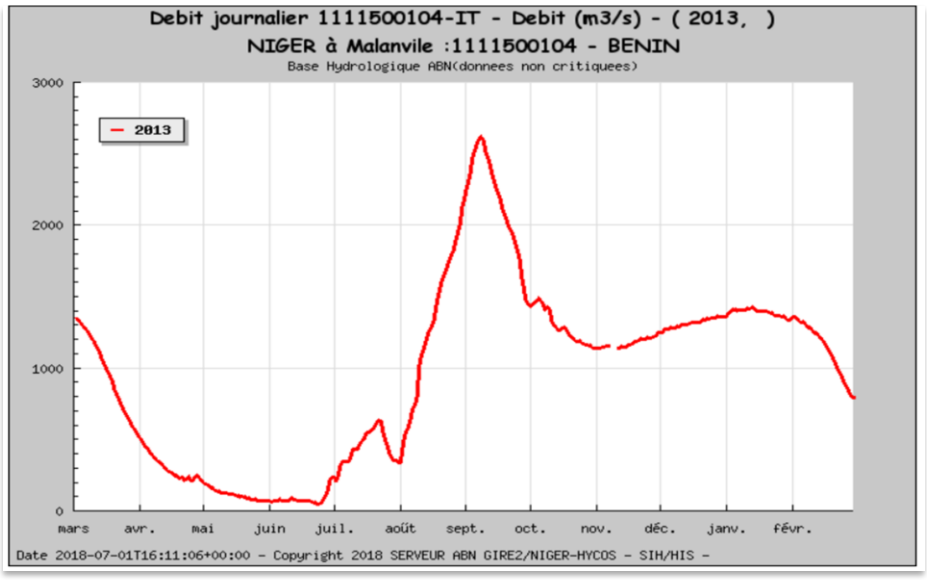

2. Measured Daily discharge (m3/s) of the Niger River at Malanville for the year 20117 (source ABN GIRE2/NIGER-HYCOS - SIH/HIS)

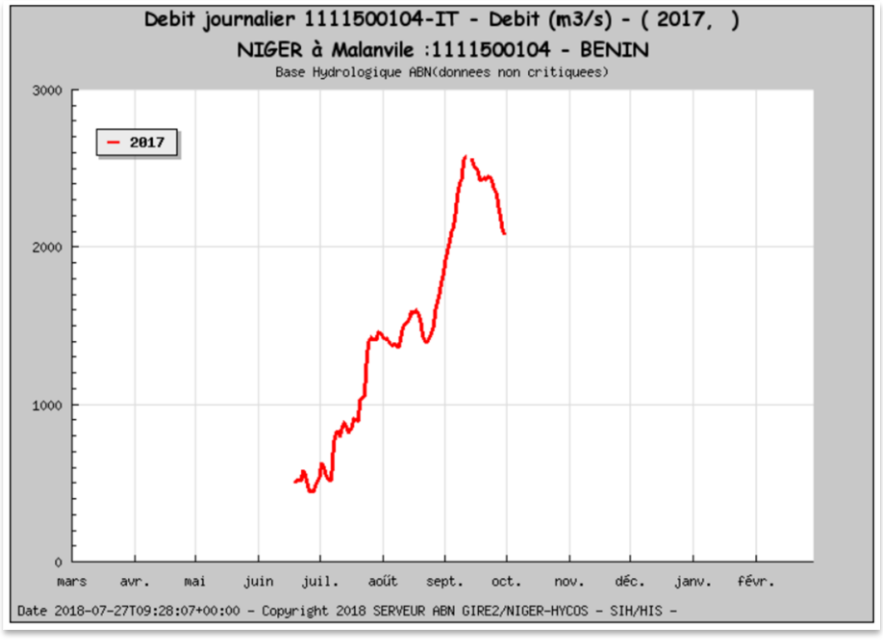

3. River geometry

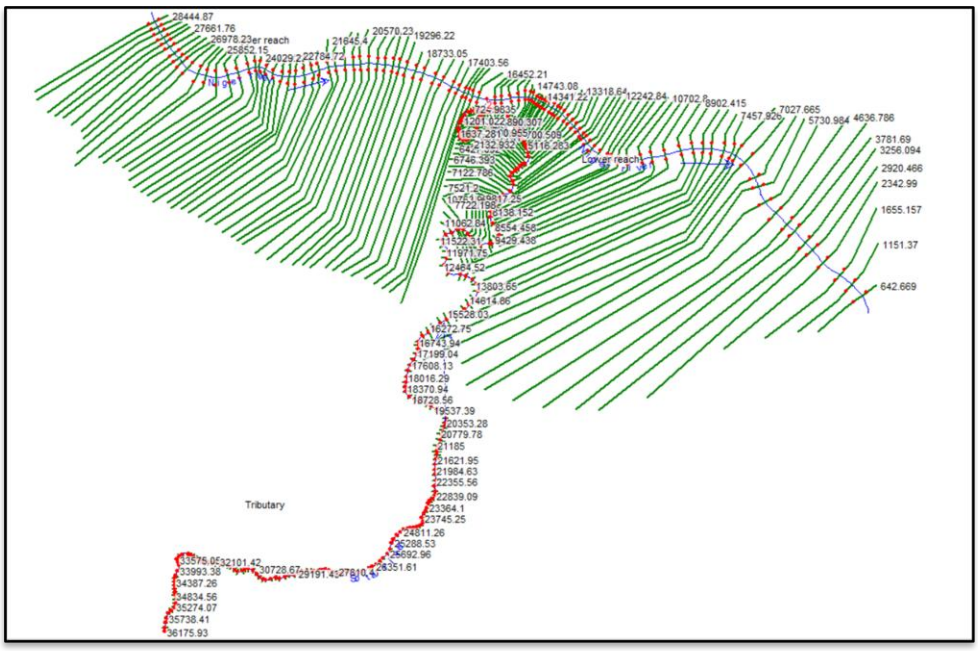

Master Thesis Expenditures

N°	Description		QTY	Unit Price	Cost per Unit Dinar DZ	Price in F CFA	Price SEK (Swedish Krona)
1	Material	office equipment (flash drive and HDD)	1	N/A	12800	N/A	N/A
2		Internet	4	1000 SEK	N/A	N/A	4000
3	Expenditures for travelling, Field work and data	Transportation in city	3	880 SEK	N/A	N/A	2640
4		Transportation Airport to city	2	150 SEK	N/A	N/A	300
5		Travel Insurance	1	7324 DZ	7324	N/A	N/A
6		Flight ticket	1	125 450 DZ	125 450	N/A	N/A
7		Cartographic Data (Land use and Shape file)	N/A	N/A	N/A	560 500	N/A
8	Printing and Binding of Thesis	Printing and Binding of Thesis	5	400 DZ	2000	N/A	N/A
Total					147 574 DZ	560 500 F CFA	6940 SEK
Total in USD					3000 USD		

Please find attached a scan copy of the receipts

Cash Receipt

Lufthansa

Reference: 2202395212881

Montant DZD: **125, 450.00**

CENT VING-CINQ
MILLE QUATRE
CENT CINQUANTE
Dinars 00 Centimes

LUFTHANSA
19 AVR. 2018
ACCUSE DE RECEPTION

19.04.2018

ENERDAS

FACTURE N° 2018/12345

ENERDAS INGENIERIE

Route Inter État Nationale 1, Cadjèhoun
02 BP 8155
Cotonou - Bénin

Le 12 Juin 2018

Client: **Modou Regis Freddy HOUNDEKINDO**

Désignation	Quantité	Prix Unitaire	Montant HT (F CFA)
Carte d'occupation des sols GIS (Municipalité de Malanville)	1	150 000	150 000
		Total	150 000
		TVA 18%	27 000
		Net à payer	177 000
ARRETE LA PRESENTE FACTURE A LA SOMME DE : **cent soixante-dix-sept mille** (177 000) **francs CFA TTC**			

PAYE

ENERDAS INGENIERIE
02 BP 8155 Cotonou - Bénin
Tel : (+229) 21 30 14 90
Fax : (+229) 21 30 01 40
RC: 2000800346, NIF 795874A
Direction

Directeur General

Caisse

Client
Divers Clients Caisse

SEDJELMACI Abdesselam
Vente de Materiel
Informatique, Communication
& Bureautique
B1 N°1 Salef el adraa-Tlemcen

N° Registre :
Mat. Fisc. :
N° Art. Impo. :

Date 21/03/2018 **N° 2634** **Page : 1**

N°	Code	Désignation	Qte	PU TTC
1	2017040401221	Disque Dur Externe 1T Segate	1	9 900.00
2	2018201866644	Pochette Disque Dur 2.5	1	0.00

Montant TTC : 9 900.00 DA

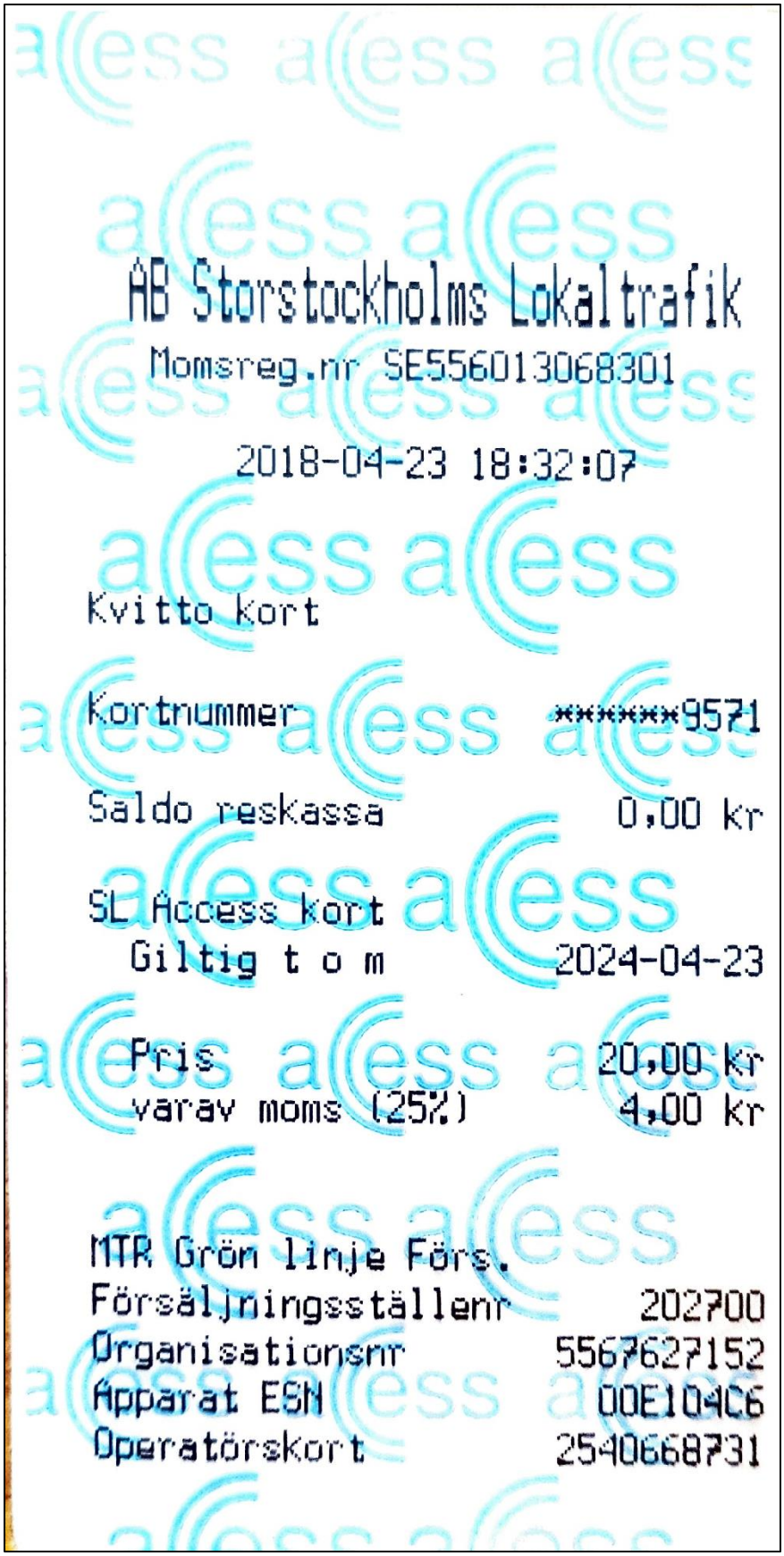

AB Storstockholms Lokaltrafik
Momsreg.nr SE556013068301

2018-04-23 18:32:07

Kvitto kort

Kortnummer	********9571
Saldo reskassa	0,00 kr
SL Access kort	
Giltig t o m	2024-04-23
Pris	20,00 kr
varav moms (25%)	4,00 kr

MTR Grön linje Förs.

Försäljningsställenr	202700
Organisationsnr	5567627152
Apparat ESN	00E104C6
Operatörskort	2540668731

Biljett/Ticket

AB Storstockholms Lokaltrafik

Enkelbiljett_vuxen

1 Vuxen

09:04, 23 apr 2018

Köpt 07:45, 23 apr 2018
Giltig till 09:04, 23 apr 2018
Pris 44 kr (6% moms 2,49 kr)
Automatnr E10C11
Biljettnr 00544

AB Storstockholms Lokaltrafik
Momsreg.nr SE556013068301

2018-04-23 07:45:43

Kvitto

Enkelbiljett_vuxen
Giltig fr o m 2018-04-23 07:45
Giltig t o m 2018-04-23 09:04

	Antal	Pris
Vuxen	1	44,00 kr
Totalt	1	44,00 kr
varav moms (6%)		2,49 kr

MTR Grön linje Förs. 202700
Försäljningsställenr 5567627152
Organisationsnr 00E10C11
Apparat ESN 2540459963
Operatörskort

Spara kvittot, det behövs vid återköp.


STOCKHOLM ARLANDA
Enkelbiljett
Ungdom, 8-25 år
SEK 150:-
One way ticket
Youth, 8-25 yrs
Giltig t.o.m.
2020-06-18
27301- rec
Inkl. 6% moms
20 MIN
ARLANDA EXPRESS

AB Storstockholms Lokaltrafik
Momsreg.nr SE556013068301

2018-04-23 18:32:15

Kvitto

Kortnummer	******9571
Saldo reskassa	0,00 kr

30-dagar vuxen

Giltighetstyp	Vid första resan
Aktiveras senast	2018-06-22

	Antal	Pris
Vuxen	1	860,00 kr

Totalt	1	860,00 kr
varav moms (6%)		48,68 kr

MTR Grön linje Förs.	
Försäljningsställenr	202700
Organisationsnr	5567627152
Apparat ESN	00E104C6
Operatörskort	2540668731

Spara kvittot, det behövs vid återköp.

AB Storstockholms Lokaltrafik
Momsreg: SE 556013068301

Kassa	91	Datum:	2018.04.23
Kvitto:	95936	Tid:	18:33

101		
Kortförsäljning		20,00
100		
30-dagar vuxen		860,00
Total		880,00
Kontant	SEK	1000,00
Växel Kontant		120,00

Moms:		
6,00 % av	860,00	48,68
25,00 % av	20,00	4,00

Trevlig resa!


201 -20 10:09
Arlanda Express
BILJETT/TICKET
Stockholm <> Arlanda
Arlanda Express SEK 150,00
Enkel Ungdom 8-25 år
Giltig 1 månad från inköp
OrgNr: 556500-3745
Kundtjänst 0771-720 200
www.arlandaexpress.com
A-Train AB:s resevilkor gäller

STOCKHOLM INFO AB

AVI ANSA EXPRESS UNGDOM 1 150,00 150,00

TOTALT SEK 150,00

KONTANT 200,00

TILLBAKA 50,00

MOMS %	MOMS	NETTO	TOTALT
3 MOMS 6%	9,49	141,51	150,00

STOCKHOLM INFO AB

ORG:NR 556741-7992

HAMNGATAN 37 11153 STOCKHOLM

08-533 37 300

VALKOMMEN ÅTER !

NI BETJÄNADES AV: KASSA 2 CENTRALEN

KONTROLL # RIHTT102901065680:FQ7CJUKEADQ2ZW37RAEAK2WPV2I

BC1Z0:LPAAFDIIKLMPCYLH7I630XNDEU

351755 15:02:46 2018-07-17 221699 2 2

amana
ليكم و لي عزاز عليكم

CONDITIONS PARTICULIER

Assurance Voyage et Assistance
Police N° : AVA5162

Le présent contrat est régi tant par l'ordonnance 95-07 du 25 Janvier 1995 relativ
06-04 du 20 février 2006, que par l'ordonnance 75/58 du 26 septembre 1975 du co
conditions particulières qui suivent :

CODE AGENCE	13G110 AGA BENMOKHTAR ABDERREZAK	**CODE PRODUIT**	051
ADRESSE	Cité des 52 Logt Imama Mansourah Tlemcen	Tél : 043 21 23 07	

DURÉE DU VOYAGE	183	Effet le : 20/04/2018	Échéance le : 19/10/2018
DESTINATION	SUEDE		Formule: Individuel

SOUSCRIPTEUR

Nom & prénom ou Raison sociale	Mr HOUNDEKINDO MODOU REGIS FREDDY		
Adresse	ROCADE 04 MANSOURAH TLM		
N° téléphone	0657-29-19-57	E-mail	

ASSURE

Nom & prénom	Mr HOUNDEKINDO MODOU REGIS FREDDY	Date de naissance	18/07/1992
Profession	Etudiant	Sexe	M
Adresse	ROCADE 04 MANSOURAH TLM TLEMCEN 13000		
N° téléphone	0657-29-19-57	E-mail	
N° du passeport	B0595266	Expire-le	10/03/2023

Garanties	Capitaux / Limites	Prime nette (DA)
Accident Corporel	200000 DA	800,00
Assistance	30000 EUR	6 234,22

Prime nette	Coût de police	Droit de timbre	Montant à payer (DA)
7 034,22	250,00	40,00	7 324,22

Fait à Tlemcen- le 04/04 /2018

Le Souscripteur
Précédée de la mention « Lu et approuvé »

L'Assureur

Agent Général
A. BENMOKHTAR

- ☐ Le souscripteur reconnaît avoir reçu un exemplaire des conditions générales et de la notice d'informations.
- ☐ Il déclare, en outre, que les informations ci-dessus sont conformes, sincères et faites de bonne foi.
- ☐ Les bénéficiaires en cas de décès accidentel sont les ayants droits.

Société d'Assurance de Prévoyance et de Santé SAPS
SPA au capital social de 1.000.000.000 de dinars algériens
40, Chemin El Mouiz Ibn Badis (Ex Poirson) El Biar, Alger 16606
RC : 11b 0987640-00/16 - NIF : 001116098764089 - NIS : 001116010171365
Tél : +213 (0) 21 790 884/885 - Fax : +213 (0) 21 790 871/873
www.amana.dz

I. G. N.

01 BP 360 COTONOU

(REP. DU BENIN)

RECU N° 129384 RECETTE N° | | | | | | | Montant CFA 383 500 FCFA

Cotonou, le 21 Juin 2018

de Mr. HOUNDEKINDO MODOU REGIS FREDDY

La somme de : Trois cent quatre-vingt trois mille cinq cents

en ESPECES CHEQUE VIREMENT

CACHET

Signature D.A.F

LIBELLE	QTE	UNITE	Montants
DONNEE CARTOGRAPHIQUE ARRONDISSEMENT (SHAPEFILE GIS) DE LA MUNICIPALITÉ DE MALANVILLE	6	35 000	210 000
DONNEE CARTOGRAPHIQUE (SHAPEFILE GIS) DEPARTEMENT DE L'ALIBORI	1	55 000	55 000
DONNEE CARTOGRAPHIQUE DU BENIN (SHAPEFILE GIS)	1	60 000	60 000

Total	**325 000**
TVA (%) (F CFA)	18%
MONTANT TTC (F CFA)	**383 500**

PAYE

Telia 1000 kr

Telia Fill 1000 kr

Serienummer: 19283704

PAFYLLNINGSKOD

3761 5760 4765 7563 5758

Så här fyller du på ditt Refill-kort:

1. Från din egen mobil. Tryck *125*
samtalskodens sifferkod # och lur. Påfyllt
belopp visas I displayen

-klart att ringa!

2. Alternativt 454 från din egen mobil
eller 020-41 10 00 från annan telefon.
Följ sedan anvisningarna.

Koden är giltig 2 är från inköpsdatum.

Vid frägor ring kundtjänst 90 200

Telia 1000 kr

Telia Fill 1000 kr

Serienummer: 19285832

PAFYLLNINGSKOD

4761 6775 2598 6512 8492

Så här fyller du på ditt Refill-kort:

1. Från din egen mobil. Tryck *125*
samtalskodens sifferkod # och lur. Påfyllt
belopp visas I displayen

-klart att ringa!

2. Alternativt 454 från din egen mobil
eller 020-41 10 00 från annan telefon.
Följ sedan anvisningarna.

Koden är giltig 2 är från inköpsdatum.

Vid frägor ring kundtjänst 90 200

Telia 1000 kr

Telia Fill 1000 kr

Serienummer: 19256473

PAFYLLNINGSKOD

3728 9308 7829 3394 1019

Så här fyller du på ditt Refill-kort:

1. Från din egen mobil. Tryck *125*
samtalskodens sifferkod # och lur. Påfyllt
belopp visas I displayen

-klart att ringa!

2. Alternativt 454 från din egen mobil
eller 020-41 10 00 från annan telefon.
Följ sedan anvisningarna.

Koden är giltig 2 är från inköpsdatum.

Vid frägor ring kundtjänst 90 200

Telia 1000 kr

Telia Fill 1000 kr

Serienummer: 19674973

PAFYLLNINGSKOD

6932 3526 4658 93034 2235

Så här fyller du på ditt Refill-kort:

1. Från din egen mobil. Tryck *125*
samtalskodens sifferkod # och lur. Påfyllt
belopp visas I displayen

-klart att ringa!

2. Alternativt 454 från din egen mobil
eller 020-41 10 00 från annan telefon.
Följ sedan anvisningarna.

Koden är giltig 2 är från inköpsdatum.

Vid frägor ring kundtjänst 90 200